Ore Geology Reviews 92 (2018) 379–396

Contents lists available at ScienceDirect

Ore Geology Reviews

journal homepage: www.elsevier.com/locate/oregeorev

Geology and mineralization at the copper-rich volcanogenic massive sulfide deposit in Nohkouhi, Posht-e-Badam block, Central Iran

Saeid Hajsadeghi[a], Mirsaleh Mirmohammadi[a,*], Omid Asghari[b], Seyed Ahmad Meshkani[a]

[a] School of Mining Engineering, University of Tehran, Tehran, Iran
[b] Simulation and Data Processing Laboratory, School of Mining Engineering, University of Tehran, Tehran, Iran

ARTICLE INFO

Keywords:
Nohkouhi
Copper rich
Volcanogenic massive sulfide
Posht-e-Badam block
Central Iran

ABSTRACT

The Nohkouhi copper deposit (1.5 Mt @ 1% Cu) is the first reported VMS deposit among several SEDEX deposits in Posht-e-Badam block, Central Iran. The deposit is primarily hosted by black shale and rhyodacite associated with Rizu Series. The Rizu Series is a volcano-sedimentary succession which was deposited in the Posht-e-Badam block during rifting of the continental margin of central Iran in the Late Precambrian to Early Cambrian. Pyrite and chalcopyrite are the dominant sulfide minerals, with subordinate galena and sphalerite. Sericite, calcite, barite, and quartz are the most abundant gangue minerals. Based on the dominance of sulfide minerals, two types of mineralization are distinguished: pyrite-rich ± chalcopyrite and chalcopyrite-pyrite rich. Considering mineralogy, the texture of sulfide mineralization, and crosscutting relationships, five ore textures are present: massive to semi-massive, laminated (banded or bedded), disseminated, brecciated, and veinlet-hosted. In the rhyodacite, sericite and carbonate are the main alteration minerals. Lithogeochemistry of felsic volcanic rocks are similar to FII rhyolite and are interpreted to have been resulted from partial melting of either continental or oceanic crust. Textural, mineralogical, and host rock alteration assemblages as well as geochemical characteristics of volcanic rocks of Nohkouhi deposit are in agreement with a copper-rich VMS deposit model.

1. Introduction

Volcanogenic massive sulfide (VMS) deposits have been studied extensively and ore-forming processes are relatively well understood (e.g. Hutchinson, 1973; Sawkins, 1976; Franklin et al., 1981, 2005; Barrie and Hannington, 1999; Galley et al., 2007; Shanks and Thurston, 2012; Tornos et al., 2015). These deposits are one of the major sources of base and precious metals in the world (Franklin et al., 1981; Barrie and Hannington, 1999). VMS deposits are formed in marine tectonic settings, including extensional oceanic seafloor spreading ridges, volcanic arcs (oceanic and continental margin), and related back-arc basin environments (e.g. Galley et al., 2007; Swinden, 1991; Syme et al., 2000; Piercey et al., 2001; Dusel-Bacon et al., 2004; Huston et al., 2010). Volcanogenic massive sulfide deposits are hosted primarily by bimodal, mafic–felsic volcanic successions (Barrie and Hannington, 1999 and Franklin et al., 2005), and have been divided into five groups by Barrie and Hannington (1999) based upon characteristic of their host successions: (1) mafic, (2) mafic-siliciclastic, (3) bimodal-mafic, (4) bimodal-felsic, and (5) felsic-siliciclastic. Also, hybrid bimodal-felsic was added as a subtype to the bimodal-felsic group by Galley et al. (2007).

Iran has various types of VMS deposits ranging in age from Ordovician to Eocene-Oligocene (Mousivand et al., 2008). The better known VMS deposits in Iran include Taknar (Karimpour and Shafaroudi, 2005), Bavanat (Mousivand et al., 2012), Chahgaz (Mousivand et al., 2011), Zurabad (Aftabi et al., 2006), Sargaz (Badrzadeh et al., 2011), Barika (Yarmohammadi et al., 2008; Khodaparast et al., 2010) and Sheikh-Ali (Rastad et al., 2002). Fig. 1 illustrates the locations of VMS and SEDEX deposits on the structural map of Iran. These deposit have different characteristics such as tectonic setting, age and metal associations.

The Nohkouhi deposit was discovered in 2011 through surface prospecting around known historical workings. Following the discovery, 19 diamond drill holes were completed and intersected 10–35 m of copper mineralization down hole. The Nohkouhi deposit contains 1.5 Mt measured resources of ore at 1% Cu (AminKarmania, 2013). There is no significant grade of other metals such as Zn, Pb, Au and Ag.

Nohkouhi is the first reported VMS and significant copper occurrence in the Posht-e-Badam block, as well as the first VMS deposit in rocks of Late Precambrian to Early Cambrian age in Iran, although several Pb-Zn SEDEX type deposits of this age are known, such as

* Corresponding author.
E-mail address: m.mirmohammadi@ut.ac.ir (M. Mirmohammadi).

https://doi.org/10.1016/j.oregeorev.2017.11.030
Received 18 September 2016; Received in revised form 12 November 2017; Accepted 27 November 2017
Available online 28 November 2017
0169-1368/

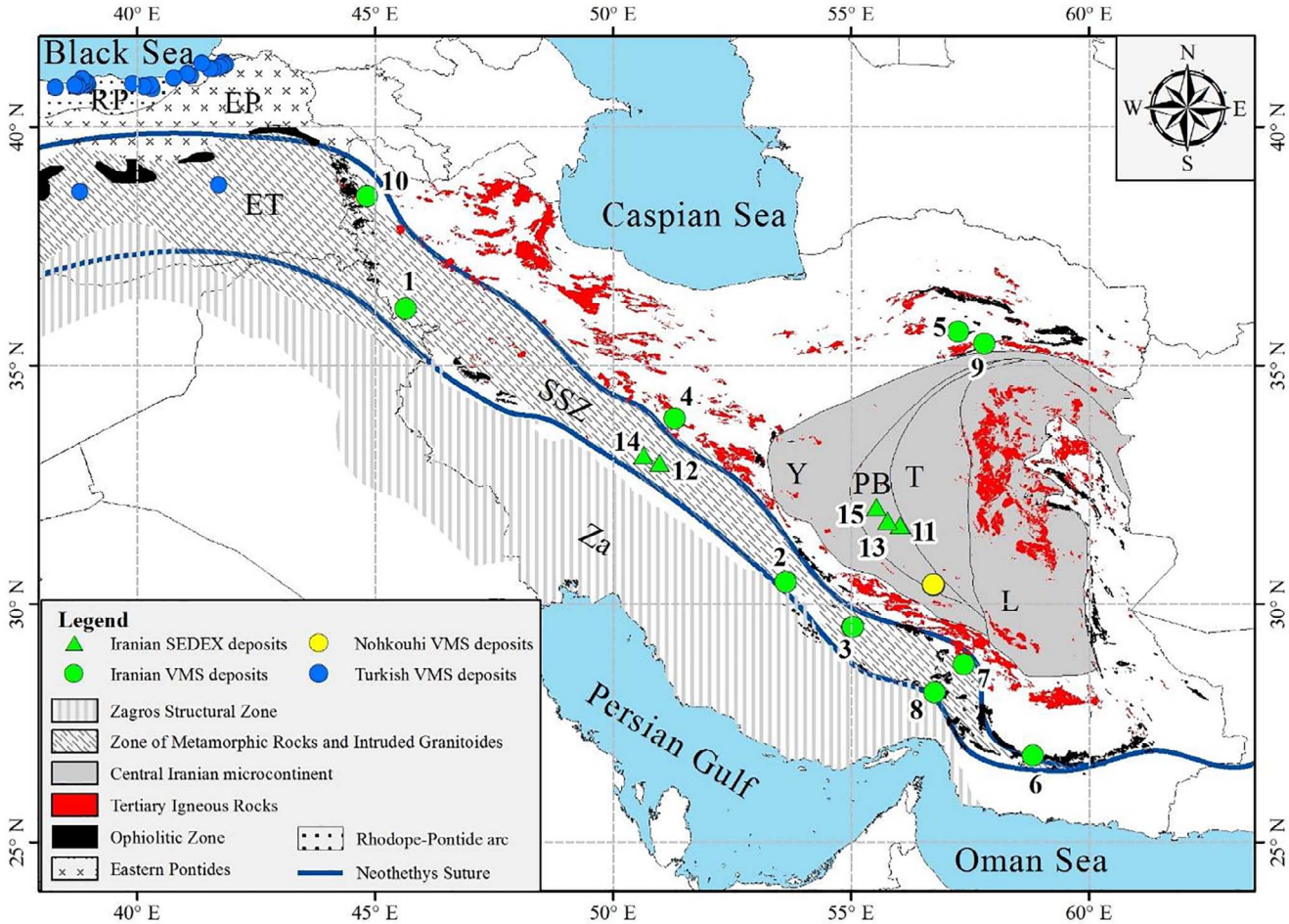

Fig. 1. Location of VMS and SEDEX deposit (from (Mousivand et al., 2008; Meshkani et al., 2013;Rajabi et al., 2015a) on structural map of Iran (Sahandi et al., 2002) and Turkey (Kuşcu et al., 2013). VMS deposit consists of: 1) Barika, 2) Bavanat, 3) Chahgaz, 4) Dorreh, 5) Nudeh, 6) Rameshk, 7) Sargaz, 8) Sheikh Ali, 9) Taknar, 10) Zurabad; and SEDEX deposit consisting 11) Chah Mir, 12) Hosein Abad, 13) Koushk, 14) Lakan, 15) Zarigan. Abbreviations: RP = Rhodope-Pontide arc, EP = Eastern Pontidus, ET = Eastern Tauride, SSZ = Sanandaj-Sirjan zone, Za = Zagros, Y = Yazd block, PB = Posht-e-Badam block, T = Tabas block, L = Lut block. Location of Nohkouhi deposit is shown with yellow circle. (For interpretation of the references to color in this figure legend, the reader is referred to the web version of this article.)

Koushk, Chahmir, and Zarigan (Rajabi et al., 2012; Rajabi et al., 2015a,b). This new discovery opens up and entire new area for VMS exploration and a detailed documentation of the Nohkouhi will contribute to improved exploration models for Cu-rich VMS deposits in Central Iran.

In this study, we describe the geology of the deposit with an emphasis on the alteration and sulfide assemblages, and on the geochemical signatures of the associated felsic volcanic rocks to establish a metallogenic model for Cu-rich VMS deposits at the regional scale.

2. Geological setting

The Nohkouhi deposit is located in the Posht-e-Badam block, a part of Central Iran microcontinent, about 70 km SE of the better known Jalal Abad iron deposit (Mehrabi et al., 2015) (Fig. 2). Central Iran is bounded by the Alborz Mountains to the north, the Lut block to the east, and the Urumieh-Dokhtar magmatic belt in the south-southwest (Ghorbani, 2013). However, the northern part of the Lut block was assumed as a part of Central Iran by Nabavi (1976). Also, based on tectono-sedimentary features, Aghanabati (2004) proposed Central Iran and Sanandaj–Sirjan zone as parts of Central Iran. Nogol Sadat (1993) suggested new subzones in his classification which extends the frontiers of Central Iran to the northeast. The formation of a rift in Central Iran is the result of extensional regime during late Precambrian to early Cambrian which produced deposits including Koushk (SEDEX: Rajabi et al., 2012), Chahmir (SEDEX: Rajabi et al., 2015a,b), Zarigan (SEDEX: Ghorbani, 2013), Angouran (mixed hypogene Zn sulfide and hypogene Zn carbonate: Daliran et al., 2013), and Alamkandi (Carbonate-hosted: Ghorbani, 2008). Fig. 3 illustrates the location of some of these deposits (e.g. Koushk, Chahmir, Zarigan), Narigan (Bonyadi and Moure, 2005) and Sehchahun (Mohseni and Aftabi, 2015) in upper Proterozoic sequences in Central Iran. Nohkouhi represents the first reported significant copper occurrence within Central Iran, and one of the very few VMS deposits outside of the Sanandaj-Sirjan zone (Fig. 1).

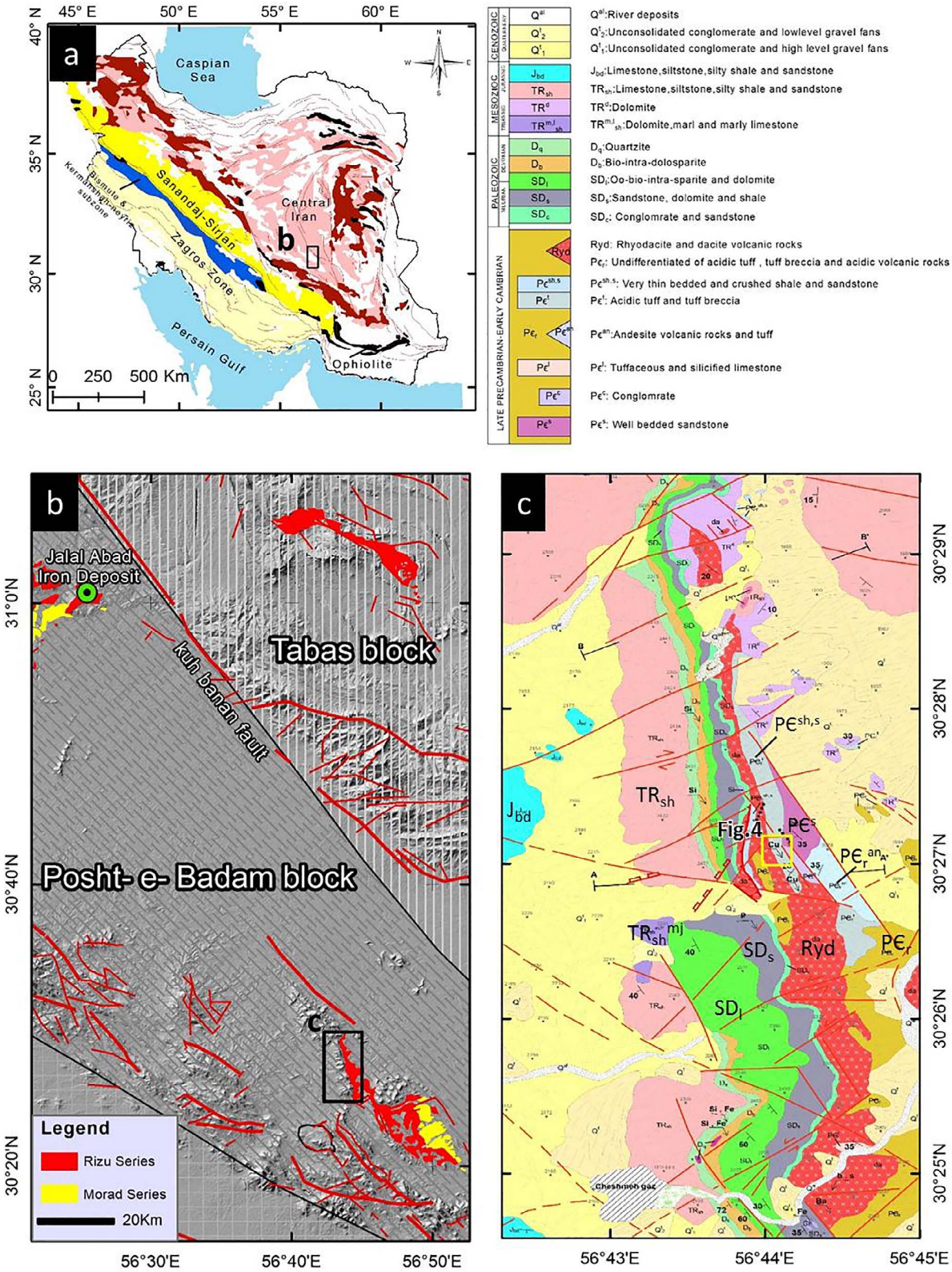

Fig. 2. Location and geological map of Nohkouhi deposit a) simplified structural zone of Iran (Nogol Sadat, 1993) b) magnification of black square b in a. Rizu Series marked by red color hosted by Jalal Abad iron deposit and Nohkouhi copper deposit based on geological map of Rafsanjan (Zohrehbakhsh et al., 1990) and Ravar (Mahdavi et al., 1996) in scale 1:250,000. c) magnification of black square c in b. Geological map of Nohkouhi deposit. (For interpretation of the references to color in this figure legend, the reader is referred to the web version of this article.)

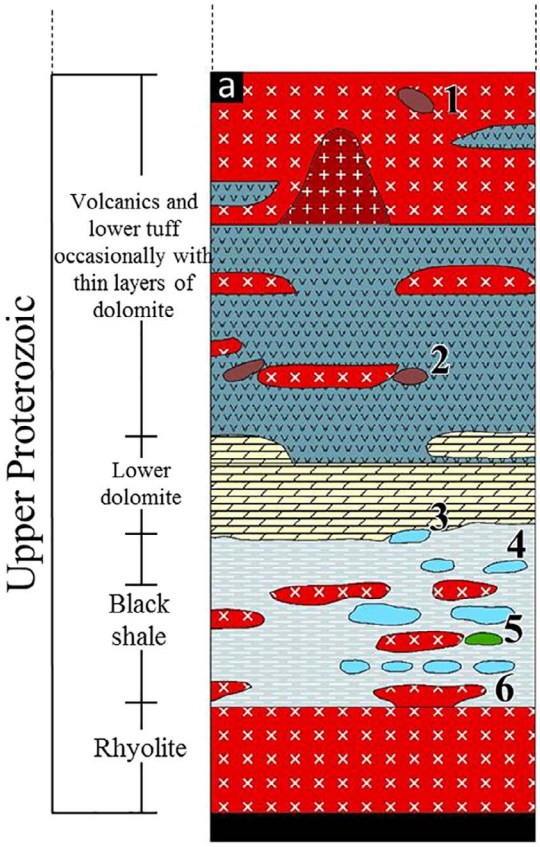

No	Deposit	Tonnage	Grade	Host rock	References
1	Sehchahun (Fe-P)	128Mt	34% Fe, 0.08% P	rhyolitic tuff, sandstone, dolomitic limestone and shale	Mohseni and Aftabi, 2015
2	Narigan (Fe-Mn)	1.4Mt	37% Fe, 5% Mn	sandy lithic tuffs, shales	Bonyadi and Moure, 2005
3	Zarigan (Pb-Zn)	-	-	Organic matter bearing calcareous black siltstone	Rajabi et al., 2015a
4	Chahmir (Zn-Pb)	1.5Mt	6% Zn, 2 % Pb	Black siltstone and shales,	Rajabi et al., 2015b
5	Nohkouhi (Cu)	1.5Mt	1% Cu	Black shale and Rhyodacite	-
6	Koushk (Zn-Pb)	5Mt	15% Zn, 3% Pb	Black siltsone, Rhyoliitic tuff	Rajabi et al., 2012

Fig. 3. a) Lithostratigraphy of upper Proterozoic rocks and mineralization associated with them modified after (Ghorbani, 2013).

The study area is bordered by Kuh Banan Fault in north and Baghin-Bafgh Fault in south. The most important faults in the area have a NW-SE general trending, which is the same trend as fold axe and copper mineralization. Second trend of faults is NE-SW. Geological units of Nohkouhi area can be divided into lower late Precambrian-early Cambrian volcano-sedimentary (Rizu Series) and upper Paleozoic, Mesozoic, and Cenozoic sedimentary. The Nohkouhi deposit is hosted in a 3–5 km wide and 16 km-long linear belt of volcano sedimentary rocks (Fig. 2c) forming the Rizu Series. The Rizu Series volcanic and sedimentary rocks were deposited in a lagoon at the time of rift initiation (Berberian and King, 1981). It unconformably overlies the Morad Series (Nairn and Alsharhan, 1997). The Rizu Formation was proposed instead of Rizu Series by Stocklin (1968). He thought that Rizu Formation is stratigraphically equivalent with Soltanieh and Barout Formations. The Rizu Series is of Late Precambrian–Early Cambrian age (Ghorbani, 2013). U-Pb zircon geochronology yields an age of 558 ± 32 Ma for the felsic volcanic rocks in Rizu Series (Al-Taha kohbanani, 1994; Darvishzadeh and Al-Taha kohbanani, 1996).

Volcanic rocks of Rizu Series originated by bimodal magmatism (Al-Taha kohbanani, 1994; Darvishzadeh and Al-Taha kohbanani, 1996). The series is comprised (bottom to top) of conglomerate, which is followed by shale, sandstone, volcanic rocks, tuffs, ferruginous dolomites, and red-brown lava (Samani, 1988). The Rizu Series hosts two ore deposits including the Jalal-Abad iron ore deposit (Mehrabi et al., 2015) (Fig. 2b) and the Homeijan magnetite-apatite deposit (Mokhtari and Ebrahimi, 2015). The Rizu Series is stratigraphically equivalent to the Early Cambrian volcano-sedimentary sequence that hosts the Chahmir zinc–lead deposit (a vent-proximal SEDEX) (Rajabi et al., 2015a,b).

On the basis of stratigraphic and geological characteristics of Rizu Series (Dostmohammadi et al., 2012), four units can be distinguished: (1) a lower sedimentary unit consisting of a thick-bedded conglomerate, (2) volcano-sedimentary units indicated by felsic lava, shale, tuff, siltstone, and sandstone with locally contains exhalative iron stone with banded texture, (3) an upper sedimentary unit constituted by thick bedded conglomerate, and (4) a rhyolite unit and breccia.

Fig. 4a shows detailed geological map of Nohkouhi deposit based on field survey. Generally, the units trend almost N—S and dip to the west. Folded and faulted black shale (light brown on weathered surface) is the main host rock of Cu mineralization. Dark brown to black rhyodacite cuts the sedimentary units. Mineralization in this rock is of lower grade than that hosted by the black shale. Unmineralized green sandstone underlies the black shale. Fig. 4b shows the geological section, provided on the map, which has been obtained by geostatistical

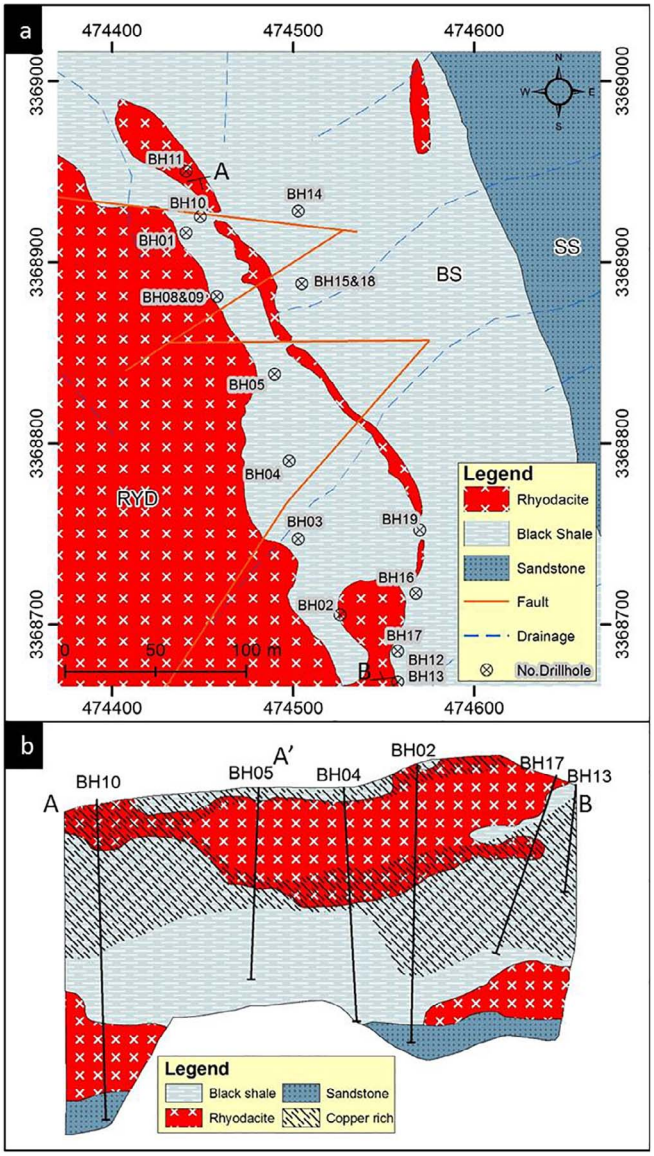

Fig. 4. (a) detailed geological map of Nohkouhi deposit including the diamond drill hole locations, (b) cross-section based on 3D geostatistical simulation of rock types (Hajsadeghi et al., 2016) and drill holes locations.

simulation of host rocks (Hajsadeghi et al., 2016). Based on successful results in VMS deposit (e.g. Schetselaar, 2013), sequential indicator simulation is applied to produce the 3D model of rock types (e.g. black shale, rhyodacite, and sandstone). The 3D geological model is constructed by calculating the most frequent occurrence of each rock unit over 30 realizations.

3. Methods of investigation

The geological map was checked by field survey and studying 20 thin and polished section. Detailed logging was reviewed and samples were selected for microscopic examinations. Documentation of the mineralogy of Nohkouhi deposit (mineralogy of host rocks alteration assemblages and ore assemblages) is based on logging of drill cores and petrographic analyses of over 20 thin and polish sections studied by using transmitted and reflected light microscopy.

To characterize chemical compositions of felsic volcanic rocks, least-altered samples were chosen according to occurrence of least alteration minerals (e.g. calcite) and intact texture by microscopic studies. They were analyzed for major, trace, and rare-earth-elements (REE). The samples were cut in half, with one half retained for archiving and the other half analyzed at Zarazma Mineral Studies Company in Tehran, Iran. Samples were crushed and pulverized in a steel mill before getting dissolved in a multi-acid solution, which is a combination of HCl (hydrochloric acid), HNO_3 (nitric acid), HF (hydrofluoric acid), and $HClO_4$ (perchloric acid). Finally, the samples were analyzed by ICP-MS. Zr were analyzed by XRF.

4. Stratigraphy and host rock petrography

The ore-bearing interval, which consists of black shale and rhyodacite, is named the Nohkouhi unit (Fig. 5). The black shale at Nohkouhi is the main host to sulfides. The black shale is laminated and contains clay minerals, chlorite, and organic matter (Fig. 6a and b). The rhyodacite is a second host but is lower grade than black shale.

The thickness of rhyodacite varies between 5 and 25 m in outcrops and between 15 and 50 m in drill holes. The rhyodacite cuts the black shale (Figs. 5c, 6e). The rhyodacite contains 15–20 vol% phenocrysts with a microporphyritic texture in a micro-to cryptocrystalline groundmass (Fig. 6c, d). According to modal analysis, phenocrysts include up to 85 vol% of quartz and plagioclase. Two other important phenocryst phases are altered mica and alkali feldspar. In some cases, there is an undifferentiated patch of black shale in rhyodacite (Fig. 6e and f). The footwall rocks consist of light brown, well-bedded sandstone and light green, tuffaceous and silicified limestone. Sandstone rocks are comprised of fine-grained quartz (up to 2 mm in diameter), feldspar, and plagioclase with medium sorting (Fig. 6 g and h). The Nohkouhi unit is overlain by undifferentiated acidic tuff, tuff breccia, and acidic volcanic rocks as well as Paleozoic sedimentary rocks.

5. Alteration

Alteration facies were identified by detailed petrographic observations of hand specimens and thin sections. Black shale is altered to sericite, chlorite and muscovite. The rhyodacite is altered to carbonate and sericite and its original texture was locally obliterated by the alteration (Fig. 7a). Fine-grained sericite is the most abundant replacement mineral at Nohkouhi. Carbonate minerals (calcite) occur mainly within fractures and as matrix in rhyodacite (Fig. 7b) and as minor replacement. Carbonate can be associated with proximal alteration zones in VMS (Lydon, 1984; Squires et al., 2001; Hudak et al., 2003; Bradshaw et al., 2008). Plagioclase is commonly replaced by sericite (Fig. 7c) and carbonate.

6. Mineralization and ore assemblage

Based on field relations, the trend of Nohkouhi ore deposit is almost N–S with a westerly dip of 25° to 30° (Fig. 3.c). The ore deposit varies in thickness from 10 to 35 m. Lateral extension of ore deposit is about 300 m. Ore body is stratabound and well zoned from copper-rich to

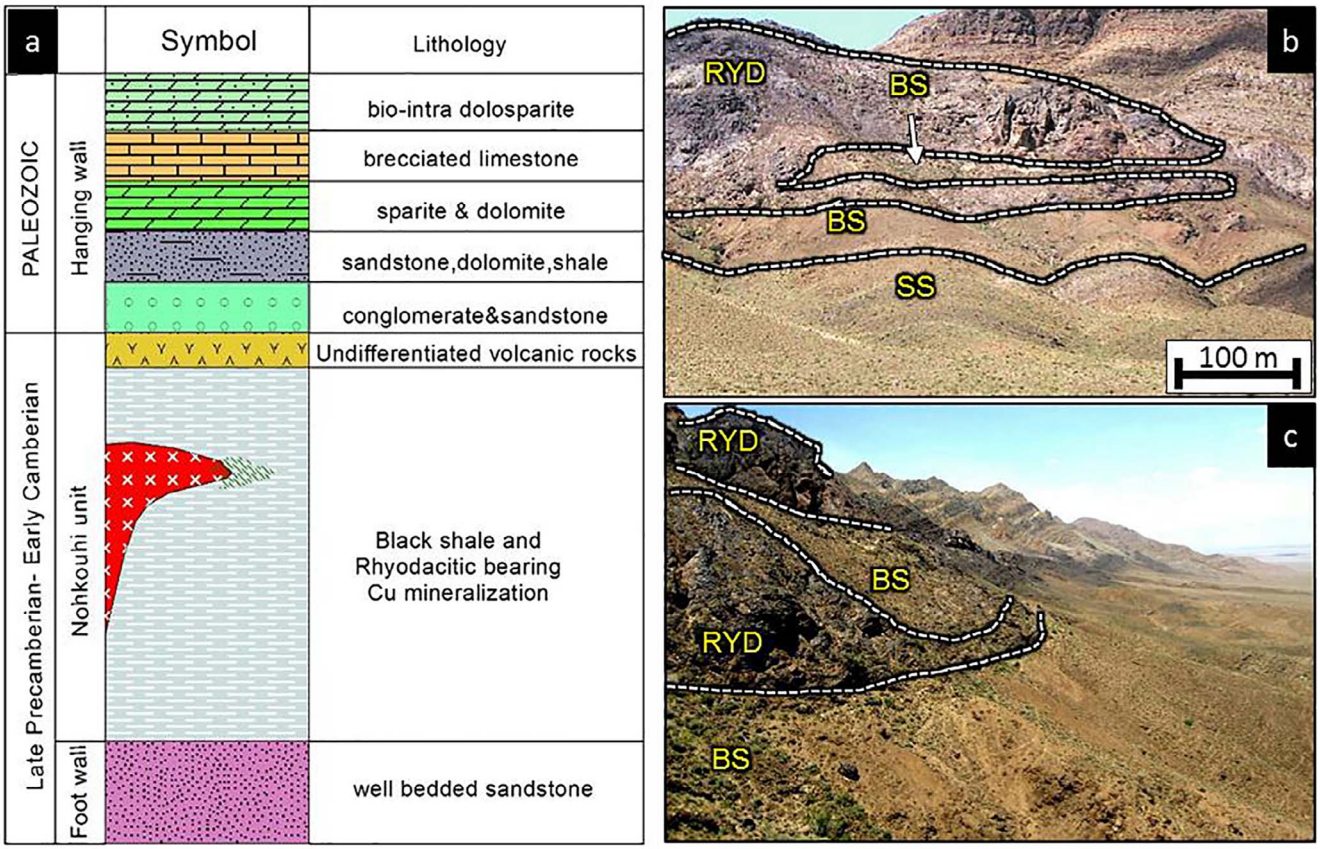

Fig. 5. a) schematic stratigraphic section of Nohkouhi deposit, b) black shale, rhyodacite, and sandstone units, view to the west, c) contact of rhyodacite and black shale, view to the north.

copper-poor.

The ore mineral assemblage of Nohkouhi deposit is simple. Sulfide minerals are dominated by pyrite and chalcopyrite, with minor sphalerite and galena. Secondary minerals include malachite, azurite, turquoise, goethite and limonite. Calcite, barite, and quartz are the most common gangue minerals.

On the basis of dominance, mineralized rocks are put in two groups: pyrite-rich ± chalcopyrite and chalcopyrite-pyrite rich. Based on ore texture, three classes are distinguished in the pyrite-rich ± chalcopyrite group, including massive to semi-massive (Fig. 8a), laminated-banded-bedded (Fig. 8b), and disseminated. Pyrite forms more than 80% of all the sulfide minerals. Pyrite exhibits two textures, framboidal and euhedral. Framboidal pyrite (Py I) is interpreted to have formed before the main mineralization and ore-forming hydrothermal stage (Fig. 8d). Pyrite is widespread in the sediments however there is a direct relationship with proximity to ore and increasing Py I. This pyrite is layered in black shale laminae (Fig. 8a–c); and texturally it occurs before the euhedral pyrite (Py II) (Fig. 8e). Framboidal pyrite has been reported in many VMS and SEDEX deposits (Constantinou and Govett, 1973; Chen, 1978; Rye et al., 1984; Koski et al., 1984; Wilkin and Barnes, 1997; Solomon and Gaspar, 2001. In the pyrite rich ± chalcopyrite group, chalcopyrite is layered with the Py I and black shale laminae, which is interpreted to show syngenetic precipitation of Ccp I, Py I and black shale in early stage. This hypothesis, supported by oxidized outcrops (Fig. 9a and b) and some microscopic evidence (Fig. 9c and d).

The Chalcopyrite-pyrite rich group is divided into five styles, including massive, semi-massive, brecciated, disseminated, and veinlet. Chalcopyrite (Ccp II) cross-cuts laminated black shale and banded Py (Py I) in most of the cases in the sulfide zone (Fig. 10a and b). Pyrite II is surrounded by chalcopyrite (Ccp II) in most of the cases and they occur in the ore-forming hydrothermal stage (Fig. 10c). Similarly, in the oxide zone malachite cuts the banded iron oxide (goethite and limonite) (Fig. 10d and e). Turquoise also occurs in the oxide zone. Digenite is presented in chalcopyrite fractures (Fig. 10c). Brecciated mineralization occurred in both black shale and rhyodacite and consists of irregular veins of pyrite, chalcopyrite, and calcite in brecciated black shale. In most cases, chalcopyrite fills the open space between euhedral pyrites.

The abundance of sulfide minerals in the rhyodacite is lower than in the black shale. In rhyodacite, chalcopyrite is present in veinlets (Fig. 11a) and as disseminated grains (Fig. 11b and c). Sphalerite is rare and is generally associated with chalcopyrite (Fig. 11d). Similarly to

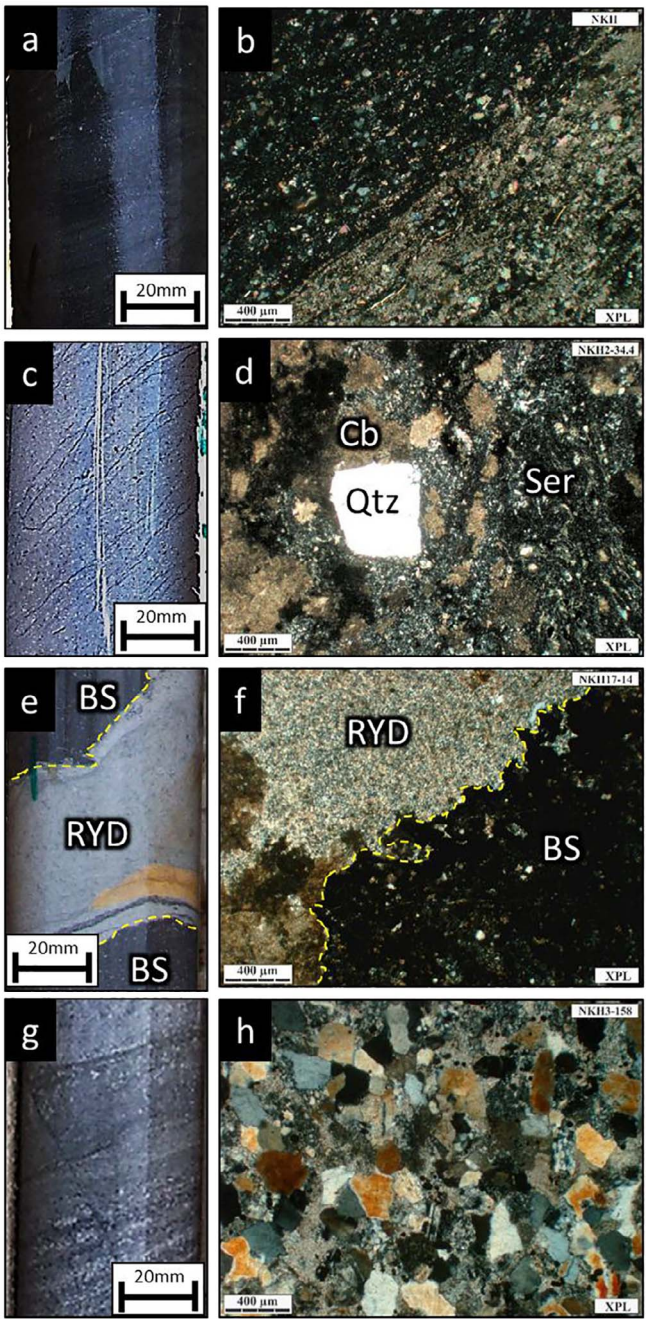

Fig. 6. Macrophotographs (a, c, e, g) and microphotographs (b, d, f, h) of rock types, (a) laminated Black shale, (b) laminated clay mineral, chlorite, and organic matter in black shale host rock, c) flow texture in rhyodacite (d) quartz phenocryst surrounded by sericitization and carbonization, (e) undifferentiated black shale and rhyodacite, (f) contact between highly altered rhyodacite and black shale, (g) layering in sandstone, h) sub-angular grains of quartz and plagioclase with medium sorting.

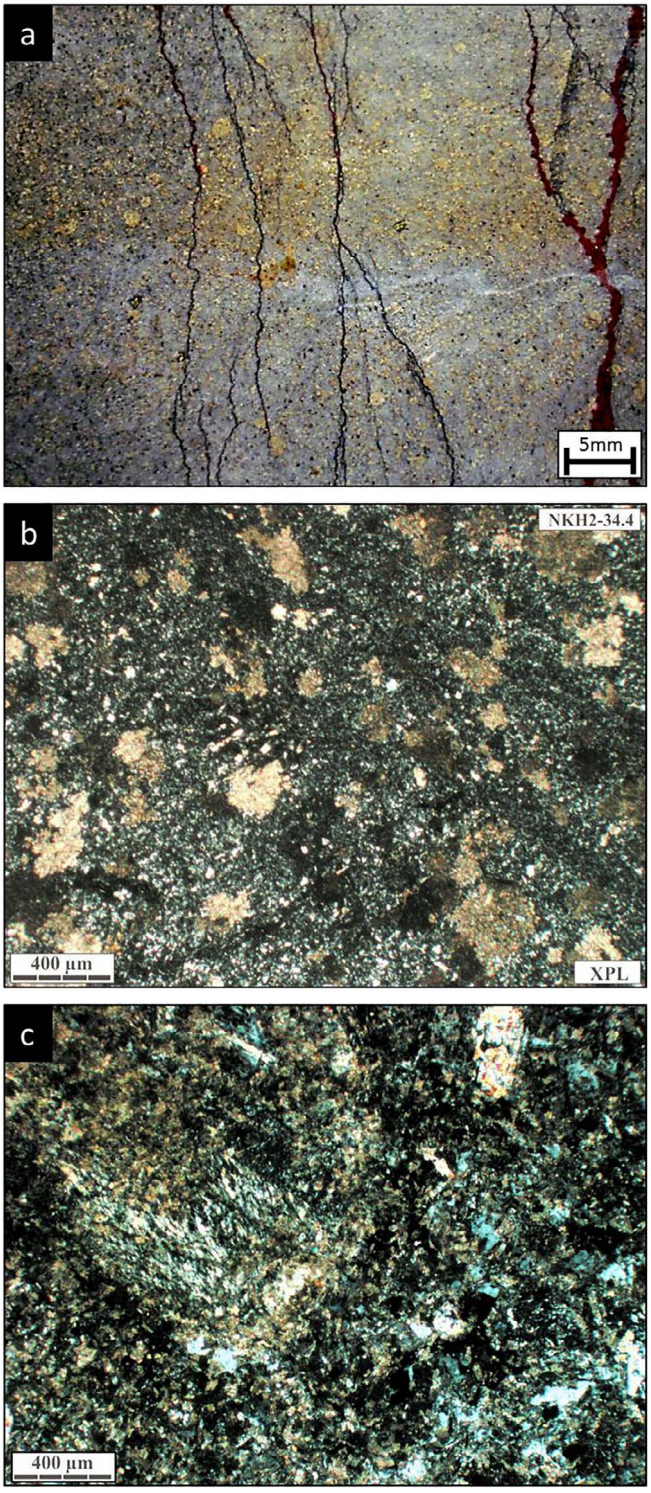

Fig. 7. Macro photographs (a) and microphotographs (b, c) of altered rhyodacite host rock; (a) carbonate alteration in rhyodacite host rock with disseminated chalcopyrite, b) carbonate alteration with opaque mineral, c) plagioclase replaced by sericite.

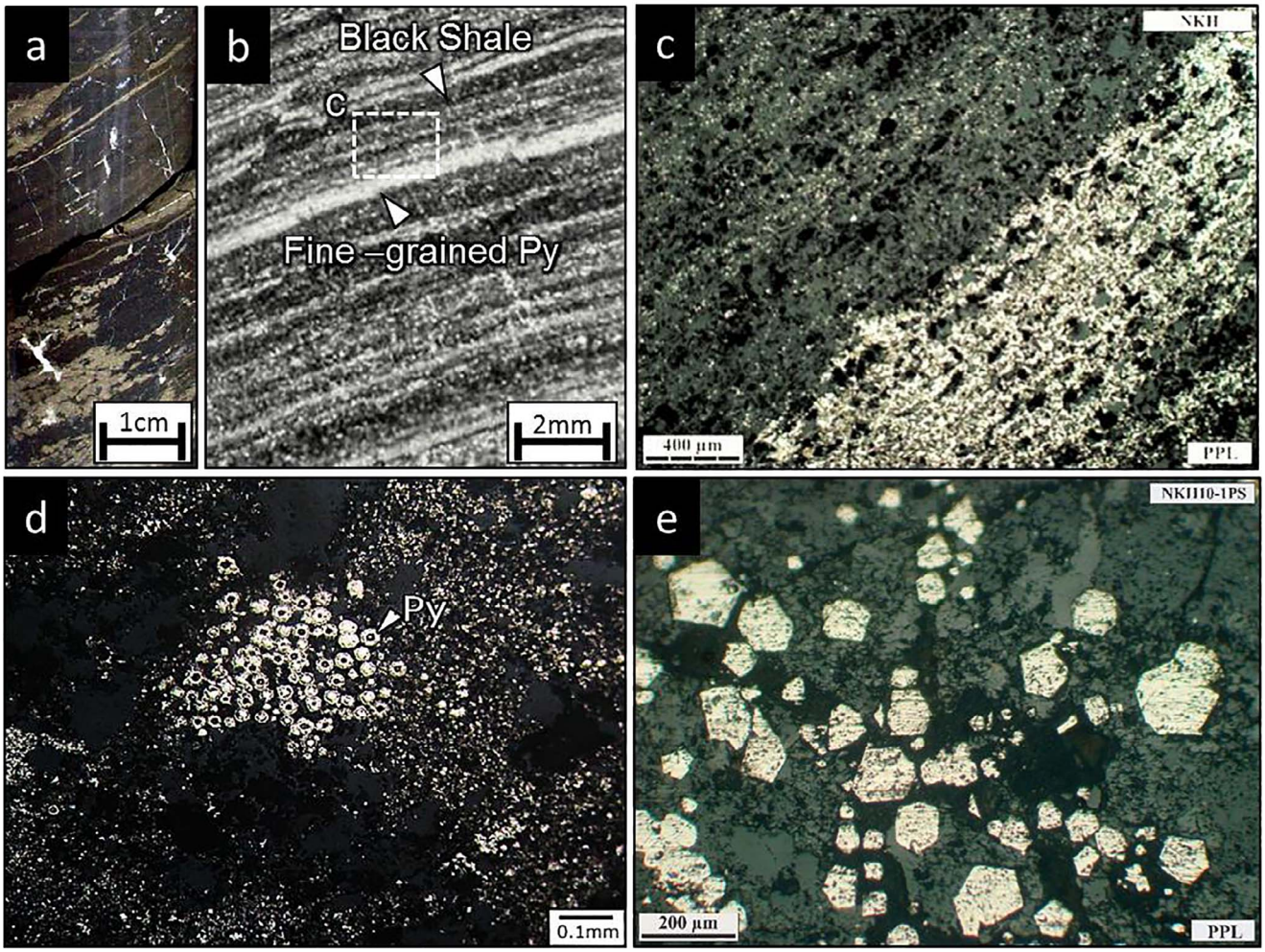

Fig. 8. Macro photographs (a, b) and microphotographs (c, d, e) of pyrite rich ± chalcopyrite group. (a) massive-semi massive pyrite in black shale, (b, c) banded pyrite (Py I) in laminated black shale shows a gradual layering in different scales without any copper mineralization. (d) framboidal Pyrite (Py I) characterizes the first stage mineralization, (e) euhedral pyrite (Py II) is formed in mineralization stage.

black shale, Py II is bordered by Ccp II (Fig. 11e).

Near surface, most sulfide minerals have been weathered to form a weathering zone that varies in thickness between 5 and10 m and contains malachite, azurite, goethite, limonite, and gypsum. This weathered zone can be divided to sub-zones of high, medium, and low intensities (Fig. 12a). At surface, rocks are strongly weathered and gypsum is formed as a result of intense weathering of pyrite (Fig. 12a). In the medium intensity zone, Mn-oxide (Fig. 12c), malachite, azurite, goethite, and limonite are formed (Fig. 12d and e). Due to weathering, the color of black shale unit changed from white to brown. In low-intensity weathering zone, digenite can be seen along fractures in chalcopyrite. There is significant upgrading in the oxidized zone.

Based on observations under the microscope, mineral textures, and crosscutting relationships, three main stages of sulfides evolution are recognized (Fig. 13a): (1) the first stage which includes the formation of Py I and Ccp I; (2) the second stage which consists of Py II, chalcopyrite, sphalerite, galena, calcite and barite that occur as massive, semi-massive, veinlet and disseminated habits (Fig. 13b and c); and (3) the third stage which consists of secondary minerals such as digenite (Fig. 13d), copper carbonate minerals (malachite, azurite, turquoise), and iron oxide and hydroxide (goethite, limonite).

7. Lithogeochemistry of felsic volcanic rocks

In the last thirty years, lithogeochemistry of volcanic rocks has become a powerful targeting tool in the exploration for VMS deposits (e.g. Lesher et al., 1986; Barrie et al., 1993; Lentz, 1998; Hart et al., 2004; Gaboury and Pearson, 2008). Combined with stratigraphic context, the geochemistry of mafic and felsic volcanic rocks can be used to outline petrochemical assemblages, which delineate potentially fertile from less fertile volcanic belts on a regional scale (Hart et al., 2004).

Petrochemical signatures related to volcanic rocks provide valuable

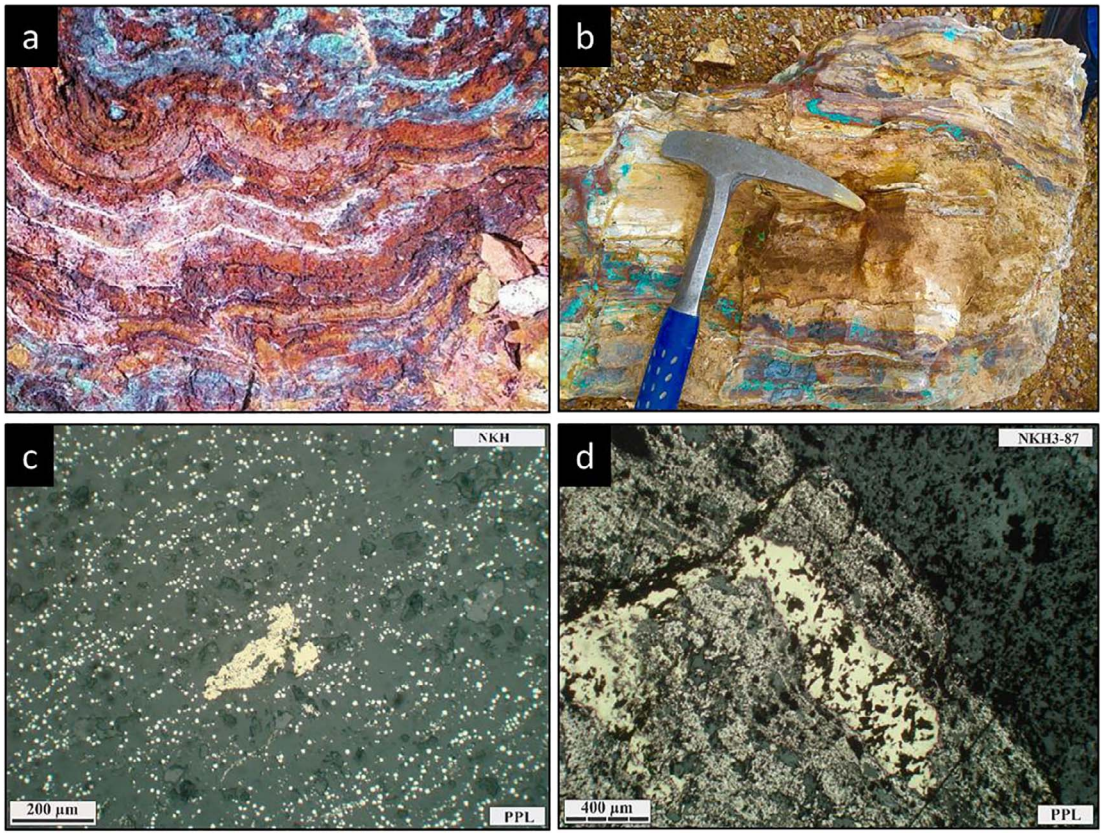

Fig. 9. Macro photographs (a, b) and microphotographs (b, c) of first stage mineralization in black shale. (a, b) copper mineralization is parallel with black shale laminae. Oxidation of sulfide minerals occurred during surface weathering, but primary texture preserved. (c, d) there is very low grade copper in Cu poor part of deposit, chalcopyrite has same trend with black shale laminae and pyrite I.

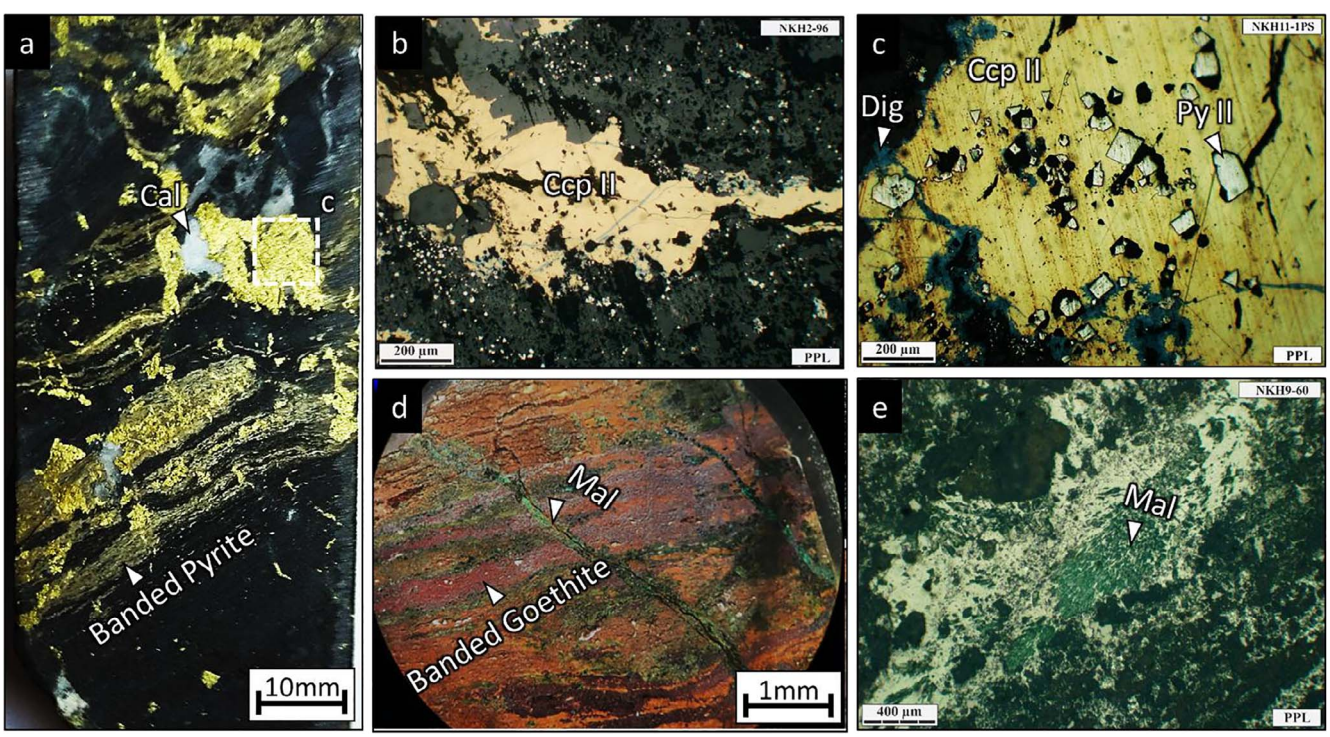

Fig. 10. Macro photographs (a) and microphotographs (b, c, d, e) of stage 2 and 3, a) banded pyrite and laminated black shale crosscut by chalcopyrite; b) magnification of white square b in a. shows chalcopyrite veinlet cut banded framboidal pyrite. c) magnification of white square, c in a digenite occurs in chalcopyrite fracture, pyrite II is surrounded by chalcopyrite. d) banded goethite and limonite crosscut by malachite in oxide zone. e) malachite veinlet cutting Fe oxide and hydroxide.

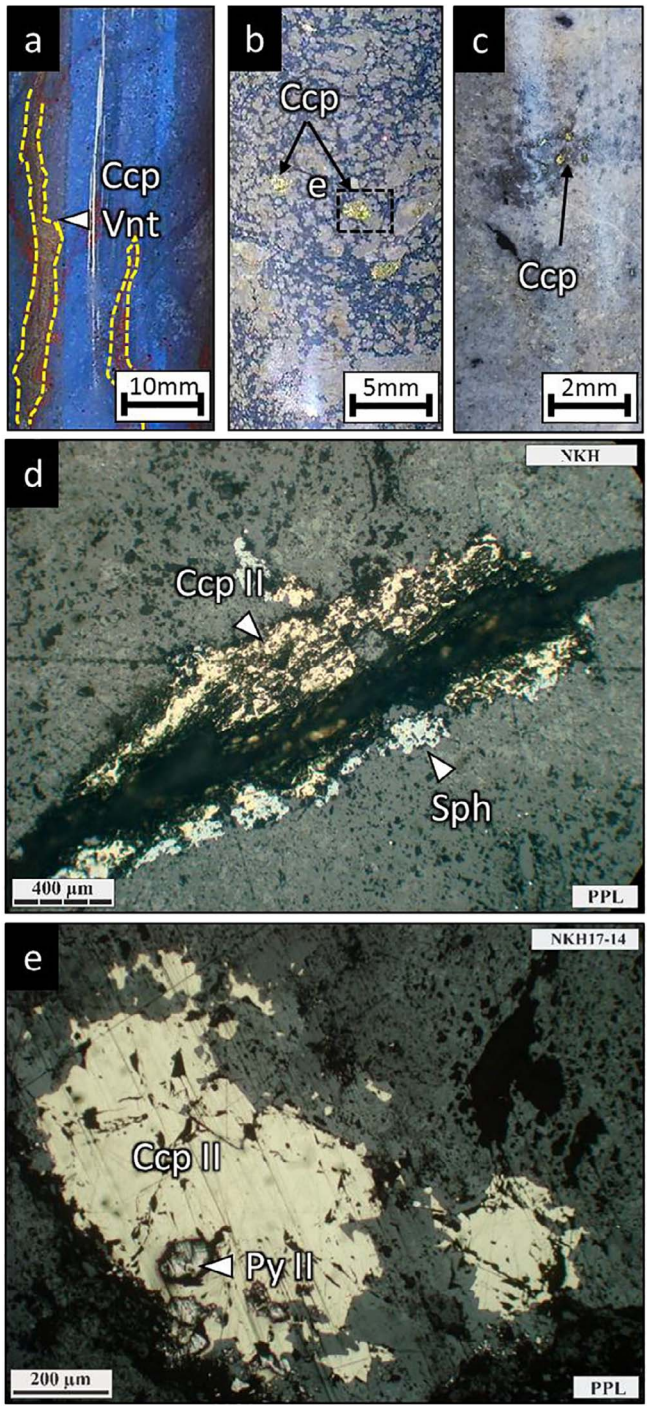

Fig. 11. Macro photographs (a, b, c) and microphotographs (d, e) of mineralization in rhyodacite, a) chalcopyrite vein in rhyodacite, b, c) disseminated chalcopyrite in rhyodacite, d) sphalerite forms around chalcopyrite. e) magnification of black square e in b, chalcopyrite surrounds euhedral pyrite.

criteria to discriminate fertile from barren prospective areas due to formation depth and tectonic setting. Felsic volcanic rocks are divided to four classes of FI, FII, FIIIa, or FIIIb types (Lesher et al., 1986; Lentz, 1998; Hart et al., 2004). According to Hart et al. (2004), FI rhyolites are unfavorable for VMS mineralization, whereas FII rhyolites predominantly host post Archean VMS deposits and FIII rhyolites host Archean VMS deposits.

A total of 14 samples from Nohkouhi area were selected for lithogeochemistry investigations. Two samples were taken from drill cores in this study. Other samples were chosen from surface outcrop of felsic volcanic rocks (Dostmohammadi et al., 2012) (see Table 1).

The Zr/Ti versus Nb/Y diagram is used to discriminate rock types (Pearce, 1996). According to Fig. 14a, samples fall within the rhyolite/dacite to alkali rhyolite field, and in the rhyolite discrimination diagram of Hart et al. (2004: Fig. 14b), the samples fall within the FII field, indicating that partial melting was likely to have taken place at moderate depths in the crust (10–15 km) (Lesher et al., 1986; Hart et al., 2004). The samples exhibit variable Zr/Y ratios, suggesting that the rocks have calc-alkaline affinities (Fig. 14c) which are matched with FII rhyolites affinities (Hart et al., 2004; Gaboury and Pearson, 2008). Nb/Y ratios (Fig. 14d) of the samples are in agreement with their formation in an arc environment or from re-melted arc crust (Lentz, 1998). REE patterns of the samples are shown in Fig. 15, and have been normalized to the chondrite values of McDonough and Sun (1995). The samples display LREE enrichment with flat HREE patterns. The FII rhyolites have gently sloping REE patterns from LREE to HREE with variable negative Eu anomalies. These cases are interpreted as arc-type rhyolites (Barrie et al., 1993; Hart et al., 2004).

8. Discussion

8.1. Style of mineralization

Volcanogenic massive sulfide deposits form in several styles, including mound style, stratiform exhalative, and sub-seafloor replacement which are described well by Tornos et al. (2015).

There are several pieces of evidence suggesting that the copper mineralization at Nohkouhi has been formed during two stages. The first stage is indicated by chalcopyrite (Ccp I) and pyrite (Py I) as a low grade stage. Ccp I and Py I are syngenetic with deposition of host rock (e.g. black shale) during submarine hydrothermal process (Fig. 9).

During second stage, copper mineralization is enriched by circulation of hydrothermal fluid in black shale and rhyodacite. During this stage, copper mineralization (Ccp II) formed by crosscutting Py I and black shale laminae (Figs. 10 and 11). Weathering was the last stage and produced oxide minerals (e.g. malachite, azurite, goethite and limonite). However, during weathering, the primary texture of sulfides preserved.

8.2. Tectonic and structural setting

VMS deposits commonly form in extensional tectonic settings, including both oceanic seafloor spreading and arc environments (Allen and Weihed, 2002; Galley et al., 2007; Piercey, 2010). Widespread 'post

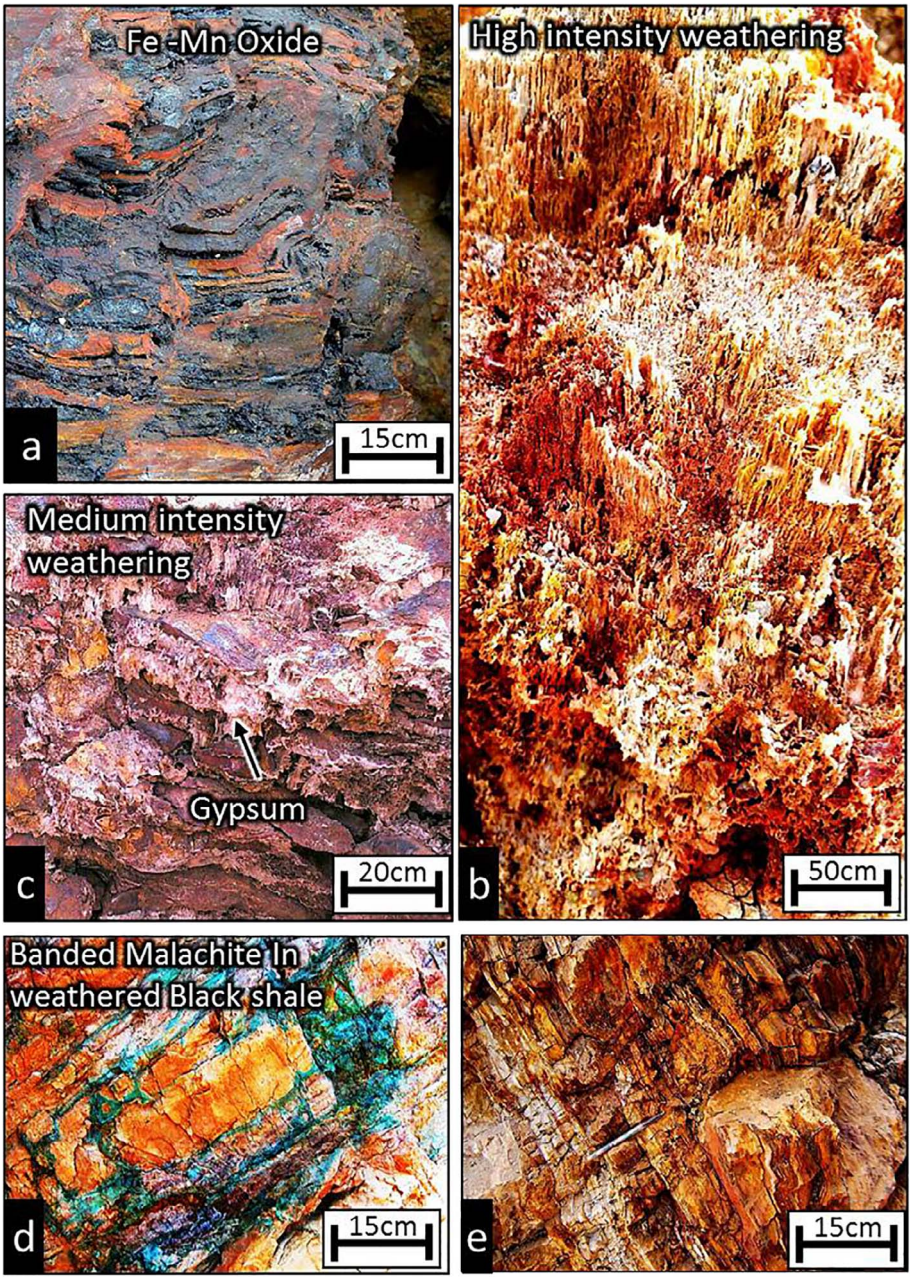

Fig. 12. Different intensities of weathering, a) Fe-Mn Oxide in high intensity weathering, b, c) gypsum and anhydrite resulting from pyrite weathering, d) banded malachite hosted by black shale in the exposed surface, e) banded Fe oxide and hydroxide leached from banded framboidal pyrite without any copper mineralization.

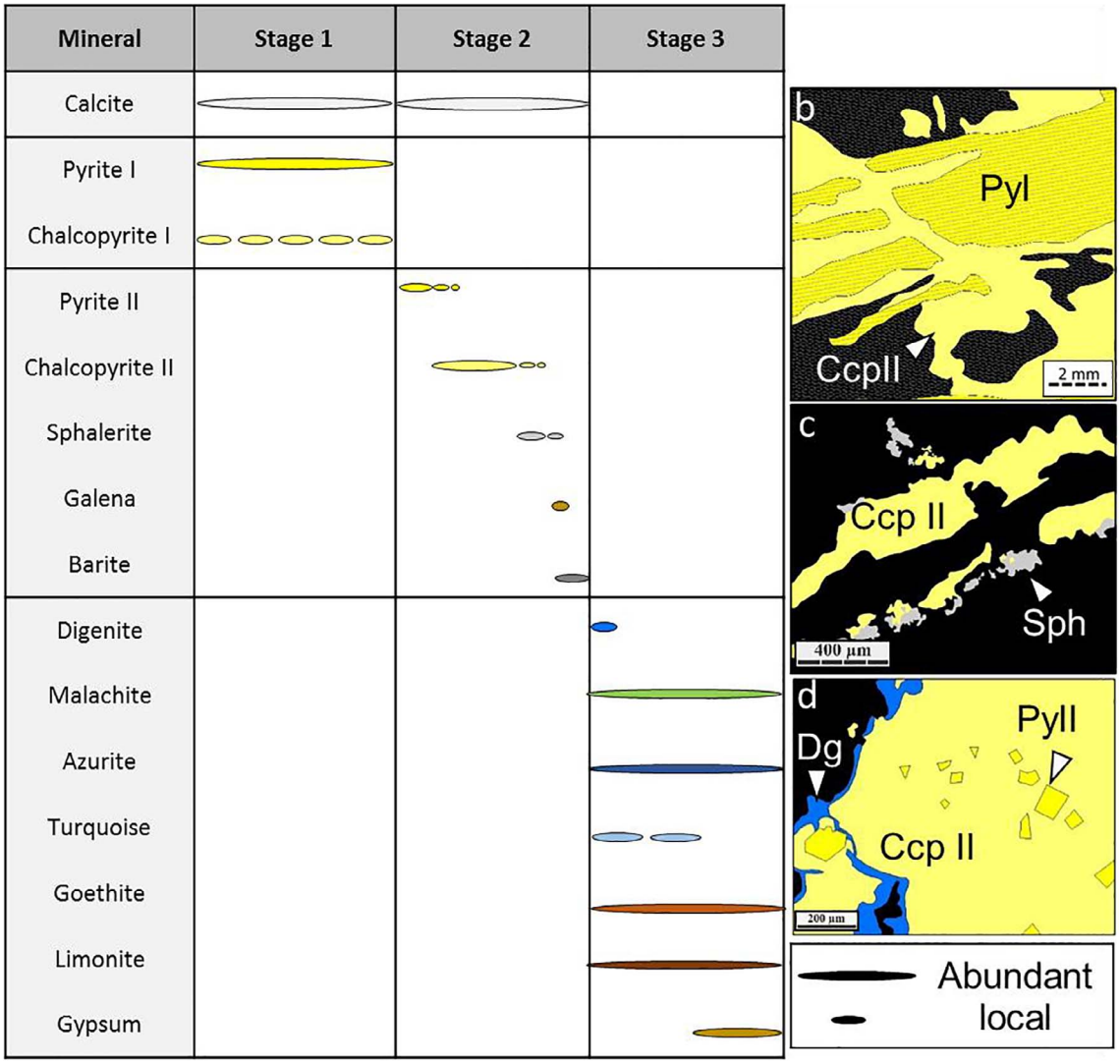

Fig. 13. (a) Mineralization paragenesis at Nohkouhi deposit, (b) chalcopyrite mineralization crosscut Py I, (c) sphalerite formed in Chalcopyrite border, (d) Py II surrounded by Chalcopyrite and Digenite formed as a secondary mineral.

Table 1
Representative analyses data for the felsic volcanic samples.

Sample/Element	Zr	Ti	La	Yb	Nb	Y
NKH-BH2	201	332	33	2.8	8.8	36
NKH-BH3	225	332	37	2.8	8.2	35
5DM-5*	154	1070	42.2	3.08	7.9	27.3
7DM-3	164	892	50.5	3.25	6.4	32.6
10DM-4	324	3807	40.5	5.25	20.7	46.9
12DM-2	65	356	16.4	2.14	4.3	17.3
13DM-1	309	3569	45.4	5.25	19.1	49.3
13DM-2	333	3867	36.6	7.59	20.4	54.6
DM-14	206	1784	90.9	3.64	11.5	33.1

Sample/Element	Ce	Pr	Nd	Sm	Eu	Gd
5DM-5	85.5	10.2	37.8	7	1.5	6.29
7DM-3	94.8	10.9	39.1	7.47	1.7	7.17
10DM-4	74.7	10.25	38.3	8.26	1.06	7.82
12DM-2	27.8	2.71	9.1	2.11	0.55	2.45
13DM-1	110.5	14	54.5	12.7	1.58	10.25
13DM-2	72.1	7.38	23.6	4.16	0.78	6.02
DM-14	123.5	11.8	36	3.8	0.84	4.38

Sample/Element	Tb	Dy	Ho	Tm	Lu
5DM-5	0.87	4.91	1.05	0.46	0.45
7DM-3	1.07	5.99	1.23	0.51	0.5
10DM-4	1.33	8.12	1.78	0.81	0.78
12DM-2	0.43	2.78	0.62	0.31	0.34
13DM-1	1.5	8.71	1.85	0.81	0.78
13DM-2	1.21	8.77	2.11	1.11	1.15
DM-14	0.77	5.16	1.21	0.55	0.55

Note: * sample with DM code from Dostmohammadi et al. (2012) analyzed by ICP-MS.

orogenic' volcanic rocks in Posht-e-Badam (Berberian and King, 1981; Samani, 1988; Talbot and Alavi, 1996) include spilitic basalts in Zarigan, Esfordi and Lakeh-Siyah areas, mafic tuffaceous rocks and rhyolitic tuffs in Koushk, Lakeh-Siyah, Narigan and Chahmir (Rajabi, 2012; Rajabi et al., 2012) reveal the bimodal magmatism which are suggested as a continental back-arc extension (Berberian and King, 1981; Samani, 1988; Talbot and Alavi, 1996; Rajabi et al., 2015a).

Rocks from the Rizu Series are among the oldest in the Posht-e-Badam block and it is mainly composed of bimodal volcanic rocks, volcano-sedimentary deposits, and dolomites (Al-Taha kohbanani, 1994; Darvishzadeh and Al-Taha kohbanani, 1996; Ghorbani, 2013). The Rizu and equivalent series (such as a Dezu series and ECVSS) are interpreted to have formed in a rift environment (Daliran, 1990; Momenzadeh and Heidari, 1995; Ghorbani, 1999, 2012). As a result, the geodynamic setting of Central Iran, especially the Posht-e-Badam block during the late Precambrian-early Cambrian, is characterized by extensional tectonic settings.

We have obtained the possible geodynamic scenario accounting for Nohkouhi deposit based on tectonic setting of the Posht-e-Badam block and the Rizu Series, the chemical signature of felsic volcanic rocks, and the style of mineralization (Fig. 16).

Continental margin back arc rifting is interpreted to have followed the subduction of oceanic crust under Central Iranian microcontinent (Rajabi et al., 2015a). Upwelling of the asthenosphere began during continental margin back arc rifting (Fig. 16a).

The mafic magmas originated from the asthenosphere and partial melting of the subduction slab. While the resulting magma ascended, differentiation and crystallization of the magma and partial melting of the upper crust formed calc-alkaline felsic magma that extruded to form of felsic volcanics (Al-Taha kohbanani, 1994; Darvishzadeh and Al-Taha kohbanani, 1996) (Fig. 16b). Felsic volcanic rocks of Nohkouhi deposit have FII chemical signatures (Fig. 12b) and they are formed as a result of partial melting of either continental or oceanic crust due to basaltic under plating during rifting (Lesher et al., 1986; Barrie et al., 1993; Barrett and MacLean, 1999; Hart et al., 2004; Piercey, 2011). Sandstone and black shale were deposited as syn-rift series (Fig. 16c). During felsic magma ascent, low grade copper (Ccp I) and laminated-banded-bedded pyrite (Py I) formed linked to submarine hydrothermal process in the initial stage of the back -arc rifting (Fig. 16d and e). Later, felsic magma intruded in black shale. Consequently, high grade copper mineralization formed in black shale by circulation of hydrothermal fluid (Fig. 16f, Table 1).

8.3. Comparison with other VMS deposits of Iran

Various types of volcanogenic massive sulfide (VMS) deposits occurred in Iran are comprised of mafic, mafic-siliciclastic, bimodal-mafic, and bimodal-felsic deposits (Mousivand et al., 2008). The vast majority of VMS deposits in Iran belong to the Cu metal associations (Fig. 17). Relevant information about these deposits is summarized in Table 2.

Several different deposits occurred during the Late Proterozoic–Early Cambrian age in Central Iran, especially in Posht-e-Badam block; they include: Sedex Pb–Zn deposits (Koushk, Chahmir, and Zarigan), magmatic and sedimentary iron oxide ore (magnetite and hematite), manganese (Anarak deposit) and magmatic phosphate, uranium, and REE (Ghorbani, 2002). Nohkouhi is the first VMS deposit in Central Iran.

Most of well-known VMS deposits in Iran are associated with ophiolite complex, including mafic type deposits such as Zurabad, Sheikh Ali, and Rameshk. These deposits occurred in Cretaceous. In fact, Cretaceous is the main period of VMS mineralization in Iran. However, other VMS deposits of Iran took place in different periods including Late Neoproterozoic (Taknar deposit), Upper Devonian or Upper Permian (Chahgaz deposit), Late Devonian-Early Carboniferous or Permo-Triassic (Bavanat deposit), Late Triassic-Early Jurassic (Sargaz deposit), and Eocene-Oligocene (Dorreh deposit) (Mousivand et al., 2008). The Nohkouhi deposit is hosted by late Precambrian-early Cambrian volcano-sedimentary series.

Volcanogenic massive sulfide deposits of Iran are medium in tonnage (2–5 Mt) and most of metal associations are Cu, Zn, Pb, Ag and Au. One of the well-known VMS deposits of Iran is Taknar (Cu-Zn-Au-Ag-Pb), a type of magnetite rich polymetallic VMS deposit. The Taknar deposit is divided into four areas called Tak I, II, III, and IV. This deposit contains 2 Mt grading 3% Cu, 1.5% Zn and 1% Pb (Karimpour and Shafaroudi, 2005). Nohkouhi is a copper-rich deposit contains 1.5 Mt ore at 1% Cu.

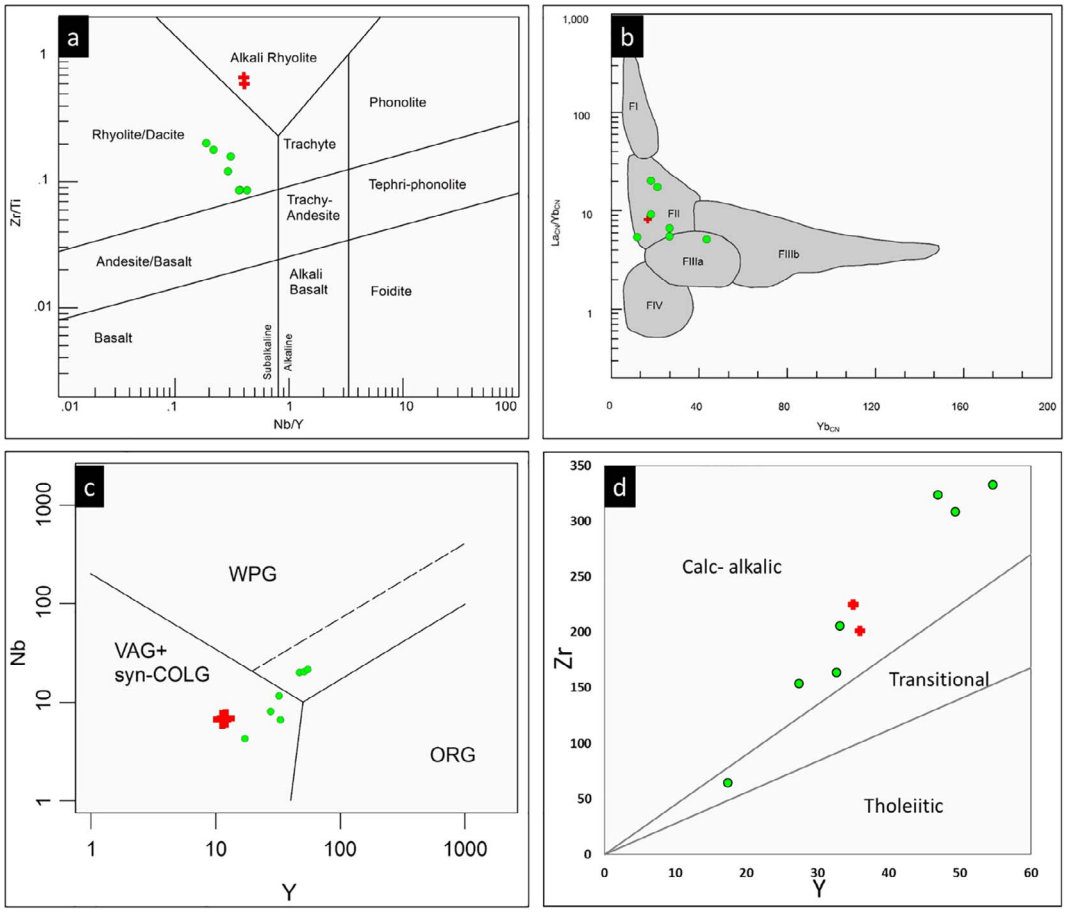

Fig. 14. Immobile element diagram for rhyolitic rocks from Nohkouhi VMS deposit (green circle from the Dostmohammadi et al. (2012) and red plus from the present study). (a) modified (Winchester and Floyd, 1977) Zr/TiO2–Nb/Y discrimination diagram for rock classification (from Pearce, 1996). (b) Lacn/Ybcn–Ybcn FI–FIV rhyolite discrimination diagram (chondrite-normalized (CN) to the values of McDonough and Sun (1995); diagrams from Lesher et al. (1986) and Hart et al. (2004). (c) Nb–Y tectonic discrimination diagram (from Pearce et al., 1984) and modified (after Dostmohammadi et al., 2012). (d) Zr–Y diagram for discriminating magma affinity (from Ross and Bédard, 2009). (For interpretation of the references to color in this figure legend, the reader is referred to the web version of this article.)

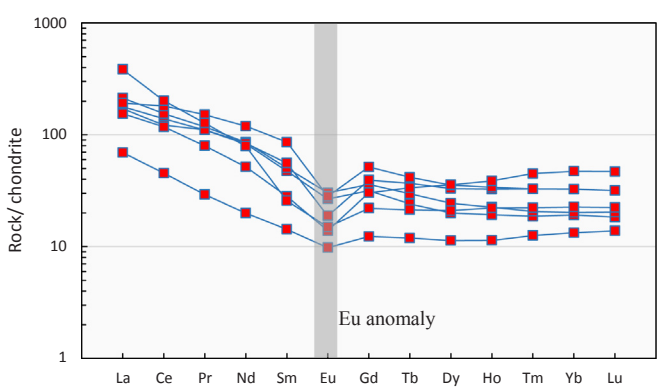

Fig. 15. Rare earth element (REE) plots of Nohkouhi deposit (chondrite-normalized (CN) to the values of McDonough and Sun (1995) and modified from Dostmohammadi et al. (2012).

8.4. Implications for regional exploration

Volcanogenic massive sulfide deposits are generally related to FII, FIII, and FIV felsic volcanic rocks in bimodal, mafic-felsic volcanic especially Archean successions (Hart et al., 2004). However, while most of FII felsic volcanic rocks are barren, some host VMS deposits (Gaboury and Pearson, 2008; Hart et al., 2004). FII felsic volcanic rocks host VMS deposits formed in bimodal volcanic successions (e.g., Bathurst: Lentz and Goodfellow, 1992; Rio Tinto: Mitjavila et al., 1997; Sturgeon Lake: Hart, 2001). As said before, Nohkouhi deposit is hosted by Rizu Series with FII felsic volcanic rocks (Fig. 14b). Rizu Series has been characterized by bimodal volcanic successions (Al-Taha kohbanani, 1994; Darvishzadeh and Al-Taha kohbanani, 1996) and this feature is interesting for more VMS explorations in Rizu and other equivalent series. The best recommendation is systematic sampling along strike in these series to identify the most intense hydrothermal signatures and to

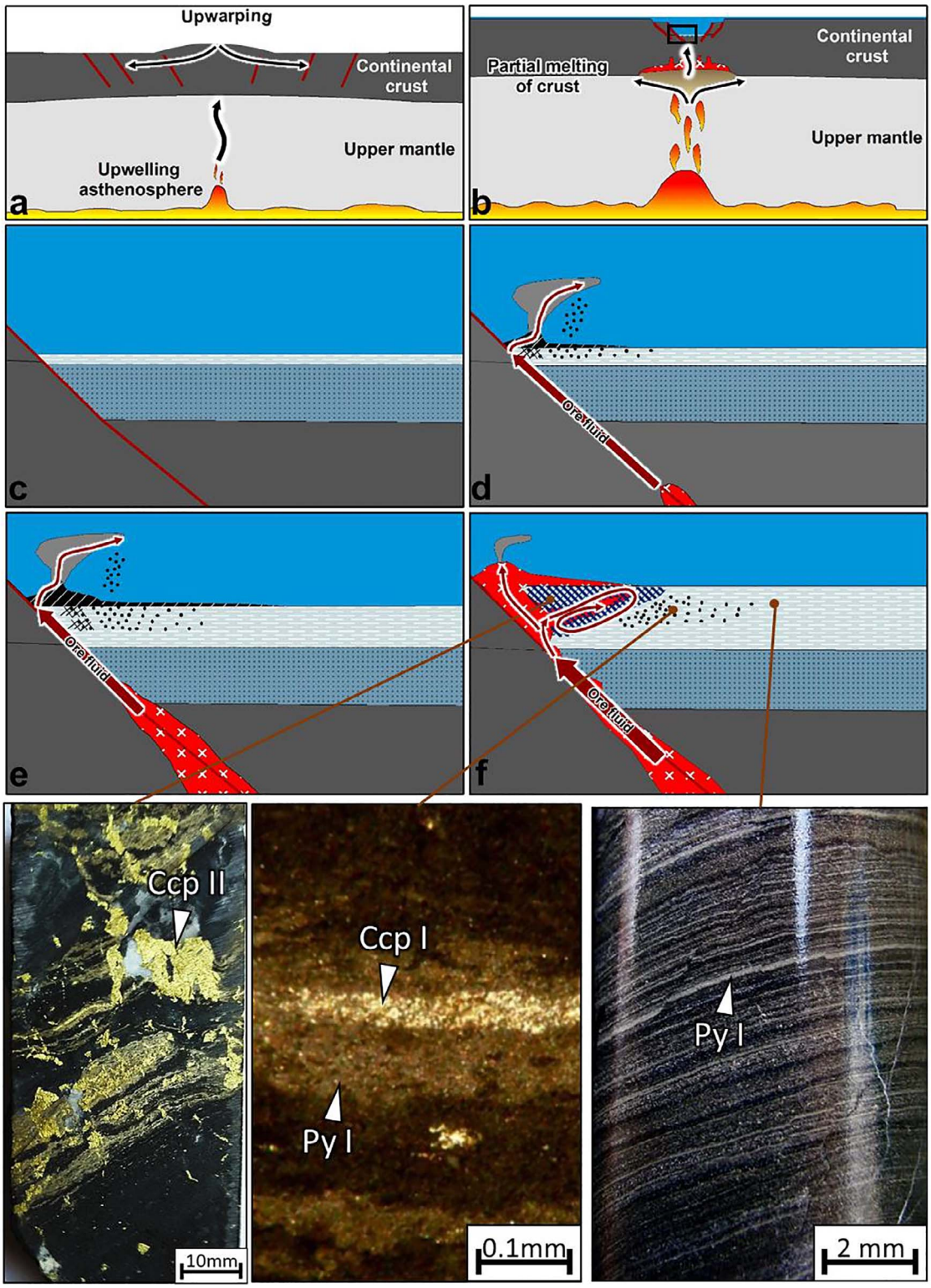

Fig. 16. Schematic block diagram illustrating possible geodynamic scenario of the formation of Nohkouhi deposit. (a) back arc rifting occurring in late Precambrian, (b) mafic rocks originating from the asthenosphere and partial melting of the upper mantle. Felsic magma as a result of partial melting of crust reached to the ground (c) sandstone and barren black shale deposited during previous episode (d, e) black shale and pyrite rich ± chalcopyrite deposited synchronously during first stage of mineralization while felsic magma ascended to the ground, (f) copper mineralization enriched as a result of circulation of magmatic fluid.

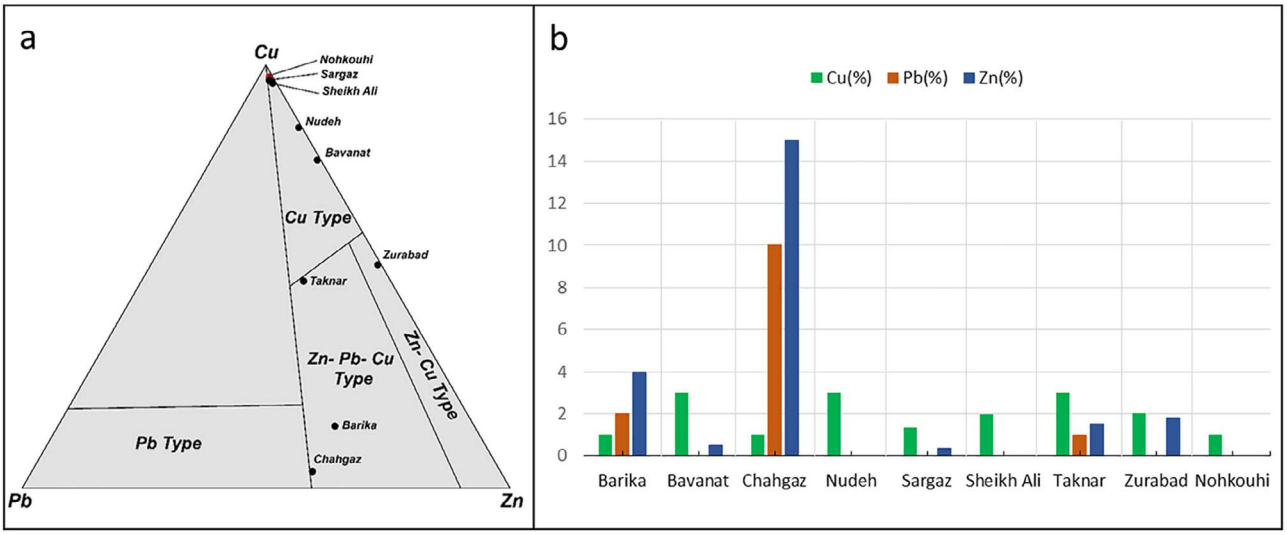

Fig. 17. (a) Cu, Pb, and Zn metal associations (Large, 1992) and (b) column bar of Cu-Pb-Zn grade of Iranian VMS deposits.

potentially locate mineralization (Lesher et al., 1986; Hart et al., 2004).

According to Nohkouhi genesis model, the same stratigraphic unit has exploration potential for VMS deposits in Central Iran, specifically in Posht-e-Badam block. Furthermore, this model leads us to pay more due attention to VMS deposits, because despite the suitable tectonic setting in Iran, VMS deposits have been explored less than porphyry Cu deposits.

In deposit scale exploration, that would be very interesting to also document any chemical modification associated with proximal alteration zones in Nohkouhi deposit as geochemical remains one of the main vectors in VMS exploration. Compositional variations of carbonate, variations in intensity of alteration minerals relative to proximity to ore can be another useful vectors in VMS exploration.

9. Conclusion

The Nohkouhi deposit is located within the Posht-e-Badam block, a part of Central Iran zone. Most of researchers emphasize the occurrence of extensional tectonic settings in Posht-e-Badam block. The host rocks of the deposit are black shale and rhyodacite associated with Rizu Series, a volcano-sedimentary series with bimodal nature and late Precambrian-early Cambrian age.

Mineralogical textures suggest that sulfide minerals are formed in three main stages: 1) a first stage characterized by framboidal pyrite and minor chalcopyrite in black shale. 2) a second stage which occurred due to intrusion of rhyodacite in black shale and enriched copper in black shale to produce euhedral pyrite and chalcopyrite, with lesser sphalerite, and galena and 3) a third stage indicated by oxidation of sulfide mineral on the exposed surface of the deposit.

The samples of felsic volcanic rocks have FII-rhyolite affinities, which suggests that the felsic volcanic rocks are generated as a result of partial melting of crust at depths between 10 and 15 km.

Given its tectonic as well as geologic setting, the type of host rock and mineralization, metal content, and lithogeochemistry of felsic volcanic rocks, Nohkouhi deposit is classified as a copper rich volcanogenic massive sulfide (VMS) deposit similar to Anyox deposit in British Columbia, Canada.

Table 2
summary of VMS deposits in Iran (deposit numbered based on Fig. 1). Deposit type based on Franklin et al. (2005).

Type	No	Deposit	Type	Structural Zone	Age	Metal associations	Tonnage and grade	References
Volcanogenic massive sulfide deposit	1	Barika	bimodal felsic	North Sanandaj-Sirjan	Cretaceous	Au-Ag (Zn-Pb-Cu)	0.5 Mt @ 4.00% Zn, 2.00% Pb, 1.00% Cu, up to 100 g/t Ag, up to 100 g/t Au	Khodaparast et al. (2010)
	2	Bavanat	Pelitic-mafic	South Sanandaj-Sirjan	Late Devonian-Early Carboniferous	Cu-Zn-Ag	6 Mt @ 3.0% Cu, 0.5% Zn, and up to 68 ppm Ag	Mousivand et al. (2012)
	3	Chahgaz	Siliciclastic felsic	South Sanandaj-Sirjan	Upper Devonian to Upper Permian	Zn-Pb-Cu	6 Mt @ 15% Zn, 10% Pb, 1% Cu, up to 100 g/t Ag, and up to 0.58 g/t Au	Mousivand et al. (2011)
	4	Dorreh	bimodal felsic	Urumieh-Dokhtar magmatic belt	Eocene-Oligocene	Ba	Not available	
	5	Nudeh	Pelitic-mafic	Sabzevar	Late Cretaceous	Cu-Zn	2 Mt @ 2–4% Cu, up to 100 g/t Ag.	Maghfouri et al. (2016)
	6	Rameshk	mafic	Makran	Cretaceous	Cu-Zn	Not available	
	7	Sargaz	bimodal mafic	South Sanandaj-Sirjan	Late Triassic to	Cu-Zn	3 Mt @ 1.34% Cu, 0.38% Zn	Badrzadeh et al. (2011)
	8	Sheikh Ali	mafic	Zagros	Cretaceous	Cu	1 Mt @ 2% Cu, 64 g/t Au	Rastad et al. (2002)
	9	Taknar	bimodal felsic	Central Iran	Late Neoproterozoic	Cu-Zn-Pb-Au-Ag	> 2 Mt @ 3% Cu, 1.5% Zn, 1.%Pb	Karimpour and Shafaroudi (2005)
	10	Zurabad	mafic	Zagros	Cretaceous	Cu (Zn)	2.8 Mt @ 2.04% Cu; 1.82% Zn	Aftabi et al. (2006)
SEDEX deposits	11	ChahMir	Vent proximal	Central Iran (Posht-e-Badam block)	Early Cambrian	Zn, Pb	1.5 Mt @ 6% Zn, 2% Pb	Rajabi et al. (2015b)
	12	Hosein Abad	–	Sanandaj-Sirjan	Jurassic	Pb, (Zn)	2 Mt @ 1% Zn, 4% Pb	Momenzadeh (1976)
	13	Koushk	Vent proximal	Central Iran (Posht-e-Badam block)	Early Cambrian	Zn-Pb	5 Mt @ 15% Zn, 3%Pb	Rajabi et al. (2012)
	14	Lakan	–	Sanandaj-Sirjan	Cretaceous	Pb, Zn, (Cu, Ag, Ba)	5 Mt @ 3% Zn, 4.5% Pb	Momenzadeh (1976)
	15	Zarigan	?	Central Iran (Posht-e-Badam block)	Early Cambrian	Pb (-Zn)	Not available	Rajabi et al. (2015a)

Acknowledgments

We would like to thank the CEO of Amin Karmania Company Mr. M.Khajoee for giving permission to access and sample the diamond drill cores. The authors are also grateful to Zarmesh group for providing the dataset used in this work. The authors especially thank Mr. A. Hazrati and Miss A. Azimian for helping to sample and take pictures of diamond drill cores. Many Thanks to Dr. David Huston and reviewers for valuable comments and suggestions which have led to improvement of this paper.

References

Aftabi, A., Ghodrati, Z., MacLean, W.H., 2006. Metamorphic textures and geochemistry of the Cyprus-type massive sulfide lenses at Zurabad, Khoy, Iran. J. Asian Earth Sci. 27 (4), 523–533.
Aghanabati, A., 2004. Geology of Iran. Geological Survey of Iran, Tehran, pp. 350 (in Persian).
Al-Taha kohbanani, B., 1994. Petrology and geochemistry of Igneous rock in east of Zarand, Kerman (Unpublished MSc. thesis). Tehran University, Tehran, Iran, pp. 117 (In Persian).
Allen, R.L., Weihed, P., 2002. Global comparisons of volcanic-associated massive sulphide districts. Geol. Soc. London Spec. Publ. 204 (1), 13–37.
AminKarmania., 2013. Company, Preliminary Exploration Report in Nohkouhi Area, Tehran, 73pp. (In Persian).
Badrzadeh, Z., Barrett, T.J., Peter, J.M., Gimeno, D., Sabzehei, M., Aghazadeh, M., 2011. Geology, mineralogy, and sulfur isotope geochemistry of the Sargaz Cu–Zn volcanogenic massive sulfide deposit, Sanandaj-Sirjan Zone, Iran. Miner. Deposita 46 (8), 905–923.
Barrett, T.J., MacLean, W.H., 1999. Volcanic sequences, lithogeochemistry, and hydrothermal alteration in some bimodal volcanic-associated massive sulfide systems. Rev. Econ. Geol. 8, 101–131.
Barrie, C.T., Hannington, M.D., 1999. Classification of volcanic-associated massive sulfide deposits based on host-rock composition. Rev. Econ. Geol. 8, 1–11.
Barrie, C.T., Ludden, J.N., Green, T.H., 1993. Geochemistry of volcanic rocks associated with Cu-Zn and Ni-Cu deposits in the Abitibi subprovince. Econ. Geol. 88 (6), 1341–1358.
Berberian, M., King, G.C.P., 1981. Towards a paleogeography and tectonic evolution of Iran. Can. J. Earth Sci. 18 (2), 210–265.
Bonyadi, Z.A.D., Moure, f., 2005. Geochemistry and genesis of Narigan ferromanganese deposit, Bafgh, Yazd province. Geosciences 15 (57), 54–63.
Bradshaw, G.D., Rowins, S.M., Peter, J.M., Taylor, B.E., 2008. Genesis of the Wolverine volcanic sediment-hosted massive sulfide deposit, Finlayson Lake District, Yukon, Canada: mineralogical, mineral chemical, fluid inclusion, and sulfur isotope evidence. Econ. Geol. 103 (1), 35–60.
Chen, T.T., 1978. Colloform and framboidal pyrite from the Caribou deposits, New Brunswick. Can. Mineral. 16 (1), 9–15.
Constantinou, G., Govett, G.J.S., 1973. Geology, geochemistry, and genesis of Cyprus sulfide deposits. Econ. Geol. 68 (6), 843–858.
Daliran, F., 1990. he magnetiteapatite deposit of Mishdovan (Unpublished PhD thesis). München University.
Daliran, F., Pride, K., Walther, J., Berner, Z.A., Bakker, R.J., 2013. The Angouran Zn (Pb) deposit, NW Iran: evidence for a two stage, hypogene zinc sulfide–zinc carbonate mineralization. Ore Geol. Rev. 53, 373–402.
Darvishzadeh, A., Al-Taha kohbanani, B., 1996. Late Precambrian magmatism and tectono magmatism in Central Iran. J. Sci. Tehran Univ. 22, 57–78 (In Persian).
Dostmohammadi, A., Ale-Taha, B., Najafzadeh, A., Nazemzadeh, M., 2012. Geochemistry and magmatism of Kuh-e AB-E-NIL igneous rock (North west of Kerman). Geochemistry 1, 24–38 (In Persian).
Dusel-Bacon, C., Wooden, J.L., Hopkins, M.J., 2004. U-Pb zircon and geochemical evidence for bimodal mid-Paleozoic magmatism and syngenetic base-metal mineralization in the Yukon-Tanana terrane, Alaska. Geol. Soc. Am. Bull. 116 (7–8), 989–1015.
Franklin, J.M., Lydon, J.W., Sangster, D.F., 1981. Volcanic-associated massive sulfide deposits. Econ. Geol. 75, 485–627.
Franklin, J.M., Gibson, H.L., Jonasson, I.R., Galley, A.G., 2005. Volcanogenic massive sulfide deposits. Economic Geology 100th Anniversary, vol. 98. pp. 523–560.
Gaboury, D., Pearson, V., 2008. Rhyolite geochemical signatures and association with volcanogenic massive sulfide deposits: examples from the Abitibi Belt, Canada. Econ. Geol. 103 (7), 1531–1562.
Galley, A.G., Hannington, M.D., Jonasson, I.R., 2007. Volcanogenic massive sulphide deposits. Mineral deposits of Canada: A synthesis of major deposit-types, district metallogeny, the evolution of geological provinces, and exploration methods: Geological Association of Canada, Mineral Deposits Division, Special Publication, vol. 5, pp.141–161.
Ghorbani, M., 1999. Chemical Properties of Magmatic Rocks of Iran, Colleague. vol. 2. Geological Survey of Iran Publication, pp. 1466.
Ghorbani, M., 2002. Economic Geology of Iran. Geological Survey of Iran Publication, pp. 700.
Ghorbani, M., 2008. Economic geology of mineral and natural resources of Iran. vol. 2 Arian Zamin Publisher 639 pp., (In Persian).
Ghorbani, M., 2012. Geology of Iran. Arian Zamin Publication, Tehran.

Ghorbani, M., 2013. Economic Geology of Iran. Springer.
Hajsadeghi, S., Asghari, O., Mirmohammadi, M., Meshkani, S.A., 2016. Indirect rock type modeling using geostatistical simulation of independent components in Nohkouhi volcanogenic massive sulfide deposit, Iran. J. Geochem. Explor. 168, 137–149.
Hart, T.R., 2001. Whole rock lithogeochemical data of prospective versus barren volcanic belts for volcanogenic massive sulphide (VMS) deposits. Superior province, Ontario: Operation treasure hunt: Ontario Geological Survey Miscellaneous Release of Data, 85.
Hart, T.R., Gibson, H.L., Lesher, C.M., 2004. Trace element geochemistry and petrogenesis of felsic volcanic rocks associated with volcanogenic massive Cu-Zn-Pb sulfide deposits. Econ. Geol. 99 (5), 1003–1013.
Hudak, G.J., Morton, R.L., Franklin, J.M., Peterson, D.M., 2003. Morphology, Distribution, and Estimated Eruption Volumes for Intracaldera Tuffs Associated with Volcanic-Hosted Massive Sulfide Deposits in the Archean Sturgeon Lake Caldera Complex, Northwestern Ontario. Explosive subaqueous volcanism, pp.345–360.
Huston, D.L., Pehrsson, S., Eglington, B.M., Zaw, K., 2010. The geology and metallogeny of volcanic-hosted massive sulfide deposits: variations through geologic time and with tectonic setting. Econ. Geol. 105 (3), 571–591.
Hutchinson, R.W., 1973. Volcanogenic sulfide deposits and their metallogenic significance. Econ. Geol. 68 (8), 1223–1246.
Karimpour, M.H., Shafaroudi, A.M., 2005. Taknar polymetal (Cu-Zn-Au-Ag-Pb) deposit: a new type magnetite-rich VMS deposit, Northeast of Iran. J. Sci., Islamic Republ. Iran 16 (3), 239–254.
Khodaparast, M., Tajedin, H., Shahrokhi, V., 2010. Nature of fluid inclusions of gold mineralization at Barika shear zone: Example of Kuroko type gold mineralization in the west of Iran. The 1st International Applied Geological Congress. Department of Geology, Islamic Azad University-Mashad Branch, Iran, pp. 26–28.
Koski, R.A., Clague, D.A., Oudin, E., 1984. Mineralogy and chemistry of massive sulfide deposits from the Juan de Fuca Ridge. Geol. Soc. Am. Bull. 95 (8), 930–945.
Kuşcu, İ., Tosdal, R.M., Gencalioğlu-Kuşcu, G., Friedman, R., Ullrich, T.D., 2013. Late Cretaceous to Middle Eocene magmatism and metallogeny of a portion of the Southeastern Anatolian orogenic belt, East-Central Turkey. Econ. Geol. 108 (4), 641–666.
Large, R.R., 1992. Australian volcanic-hosted massive sulfide deposits; features, styles, and genetic models. Econ. Geol. 87 (3), 471–510.
Lentz, D.R., 1998. Petrogenetic evolution of felsic volcanic sequences associated with Phanerozoic volcanic-hosted massive sulphide systems: the role of extensional geodynamics. Ore Geol. Rev. 12 (5), 289–327.
Lentz, D. and Goodfellow, W., 1992. Re-evaluation of the petrochemistry of felsic volcanic and volcaniclastic rocks near the Brunswick no. 6 and 12 massive sulfide deposits, Bathurst mining camp, New Brunswick. Current Research, part E, Geological Survey of Canada Paper, 92, pp.343–350.
Lesher, C.M., Goodwin, A.M., Campbell, I.H., Gorton, M.P., 1986. Trace-element geochemistry of ore-associated and barren, felsic metavolcanic rocks in the Superior Province, Canada. Can. J. Earth Sci. 23 (2), 222–237.
Lydon, J.W., 1984. Volcanogenic sulphide deposits, part 1, a descriptive model. Geosci. Can. 11, 195–202.
Maghfouri, S., Rastad, E., Mousivand, F., Lin, Y., Zaw, K., 2016. Geology, ore facies and sulfur isotopes geochemistry of the Nudeh Besshi-type volcanogenic massive sulfide deposit, southwest Sabzevar basin, Iran. J. Asian Earth Sci. 125, 1–21.
Mahdavi, M.A., Soheili, M., Mohajel, M., Huckriede, R., Haj mola ali, A., 1996. Geology Map of Ravar, Scale 1:250,000. Geological Survey of Iran.
McDonough, W.F., Sun, S.S., 1995. The composition of the Earth. Chem. Geol. 120 (3), 223–253.
Mehrabi, B., Shahraki, B.K., Guilani, K.B., Masoudi, F., 2015. Early Cambrian high-temperature dolomite of the Rizu Series in the Jalal-Abad iron ore deposit, Central Iran. Arabian J. Geosci. 8 (9), 7163–7176.
Meshkani, S.A., Mehrabi, B., Yaghubpur, A., Sadeghi, M., 2013. Recognition of the regional lineaments of Iran: Using geospatial data and their implications for exploration of metallic ore deposits. Ore Geol. Rev. 55, 48–63.
Mitjavila, J., Marti, J., Soriano, C., 1997. Magmatic evolution and tectonic setting of the Iberian Pyrite Belt volcanism. J. Petrol. 38 (6), 727–755.
Mohseni, S., Aftabi, A., 2015. Structural, textural, geochemical and isotopic signatures of synglaciogenic Neoproterozoic banded iron formations (BIFs) at Bafq mining district (BMD), Central Iran: the possible Ediacaran missing link of BIFs in Tethyan metallogeny. Ore Geol. Rev. 71, 215–236.
Mokhtari, M.A.A., Ebrahimi, M., 2015. Geology and geochemistry of Homeijan magnetite-Apatite deposit (SW Behabad, Yazd province). Geochem. J. 2, 20–27.
Momenzadeh, M., 1976. Stratabound lead-zinc ores in the lower Cretaceous and Jurassic sediments in the Malāyer-Esfahan district (west central Iran): lithology, metal content, zonation and genesis (Doctoral dissertation).
Momenzadeh, M., Heidari, E., 1995. Ore-hydrocarbon resources and alkaline magmatism of Late Proterozoic-Early Cambrian in Iran: a genetic interpretation. Carbonates Evaporites 10 (1), 79–88.
Mousivand, F., Rastad, E., Peter, M., 2008. An overview of volcanogenic massive sulfide deposits of Iran. In 33rd Int Geol Congress, Oslo.
Mousivand, F., Rastad, E., Meffre, S., Peter, J.M., Solomon, M., Zaw, K., 2011. U-Pb geochronology and Pb isotope characteristics of the Chahgaz volcanogenic massive sulphide deposit, southern Iran. Int. Geol. Rev. 53 (10), 1239–1262.
Mousivand, F., Rastad, E., Meffre, S., Peter, J.M., Mohajjel, M., Zaw, K., Emami, M.H., 2012. Age and tectonic setting of the Bavanat Cu–Zn–Ag Besshi-type volcanogenic massive sulfide deposit, southern Iran. Miner. Deposita 47 (8), 911–931.
Nabavi, M., 1976. An introduction to geology of Iran. Geological Survey of Iran, Tehran.
Nairn, A.E.M., Alsharhan, A.S., 1997. Sedimentary Basins and Petroleum Geology of the Middle East. Elsevier.
Nogol Sadat, M.M.A., 1993. Tectonic map of Iran, treatise on the geology of Iran. Ministry of Mines and Metals, Tehran.
Pearce, J.A., 1996. A user's guide to basalt discrimination diagrams. Trace element geochemistry of volcanic rocks: applications for massive sulphide exploration. Geol. Assoc. Can. 12 (79), 113 Short Course Notes.
Pearce, J.A., Harris, N.B., Tindle, A.G., 1984. Trace element discrimination diagrams for the tectonic interpretation of granitic rocks. J. Petrol. 25 (4), 956–983.
Piercey, S.J., 2010. An overview of petrochemistry in the regional exploration for volcanogenic massive sulphide (VMS) deposits. Geochem. Explor. Environ. Anal. 10 (2), 119–136.
Piercey, S.J., 2011. The setting, style, and role of magmatism in the formation of volcanogenic massive sulfide deposits. Miner. Deposita 46 (5–6), 449–471.
Piercey, S.J., Paradis, S., Murphy, D.C., Mortensen, J.K., 2001. Geochemistry and paleotectonic setting of felsic volcanic rocks in the Finlayson Lake volcanic-hosted massive sulfide district, Yukon, Canada. Econ. Geol. 96 (8), 1877–1905.
Rajabi, A., 2012. Ore controlling parameters and genesis of sedimentary-exhalative Zn-Pb (SEDEX type) deposits, Zarigan-Chahmir Area, East of Bafq, Central Iran (Unpublished Ph. D. thesis). Tarbiat Modares University, Iran, pp. 420.
Rajabi, A., Rastad, E., Alfonso, P., Canet, C., 2012. Geology, ore facies and sulphur isotopes of the Koushk vent-proximal sedimentary-exhalative deposit, Posht-e-Badam Block, Central Iran. Int. Geol. Rev. 54 (14), 1635–1648.
Rajabi, A., Canet, C., Rastad, E., Alfonso, P., 2015a. Basin evolution and stratigraphic correlation of sedimentary-exhalative Zn–Pb deposits of the Early Cambrian Zarigan-Chahmir Basin, Central Iran. Ore Geol. Rev. 64, 328–353.
Rajabi, A., Rastad, E., Canet, C., Alfonso, P., 2015b. The early Cambrian Chahmir shale-hosted Zn–Pb deposit, Central Iran: an example of vent-proximal SEDEX mineralization. Miner. Deposita 50 (5), 571–590.
Rastad, E., Miralipour, A.M., Momenzadeh, M., 2002. Sheikh-ali copper deposit, a Cyprus-type VMS deposit in southeast Iran. J. Sci. Islam. Repub. Iran 13, 51–63.
Ross, P.S., Bédard, J.H., 2009. Magmatic affinity of modern and ancient subalkaline volcanic rocks determined from trace-element discriminant diagrams. Can. J. Earth Sci. 46 (11), 823–839.
Rye, R.O., Roberts, R.J., Snyder, W.S., Lahusen, G.L., Motica, J.E., 1984. Textural and stable isotope studies of the Big Mike cupriferous volcanogenic massive sulfide deposit, Pershing County, Nevada. Econ. Geol. 79 (1), 124–140.
Sahandi, M.R., Soheily, M., Sadeghi, M., Delavar, S.T., Jafari Rad, A., 2002. Geological Map of Iran, 1:1,000,000. Geological Survey of Iran, Tehran Unpublished.
Samani, B.A., 1988. Metallogeny of the Precambrian in Iran. Precambrian Res. 39 (1), 85–106.
Sawkins, F.J., 1976. Massive sulphide deposits in relation to geotectonics. Metallogeny and Plate Tectonics. Geological Association of Canada, pp. 221–240 Spec. Paper, 14,.
Schetselaar, E.M., 2013. Mapping the 3D lithofacies architecture of a VMS ore system on a curvilinear-faulted grid: A case study from the Flin Flon mining camp, Canada. Ore Geol. Rev. 53, 261–275.
Shanks, W.C., Thurston, R. (Eds.), 2012. Volcanogenic Massive Sulfide Occurrence Model. US Department of the Interior, US Geological Survey.
Solomon, M., Gaspar, O.C., 2001. Textures of the Hellyer volcanic-hosted massive sulfide deposit, Tasmania—the aging of a sulfide sediment on the sea floor. Econ. Geol. 96 (7), 1513–1534.
Squires, G.C.S., Brace, T.D., Hussey, A.M., 2001. Newfoundland's polymetallic Duck Pond Deposit: earliest Iapetan VMS mineralization, formed within a sub-seafloor, carbonate-rich alteration system. In Geology and mineral deposits of the Northern Dunnage Zone, Newfoundland Appalachians. Edited by DTW Evans and A. Kerr. Geological Association of Canada-Mineralogical Association of Canada (GAC–MAC) Annual Meeting, St. John's, Nfld, pp. 167–187.
Stocklin, J., 1968. Structural history and tectonics of Iran: a review. AAPG Bull. 52 (7), 1229–1258.
Swinden, H.S., 1991. Paleotectonic settings of volcanogenic massive sulphide deposits in the Dunnage Zone, Newfoundland Appalachians. CIM Bull. 84 (946), 59–69.
Syme, E.C., Lucas, S.B., Bailes, A.H., Stern, R.A., 2000. Contrasting arc and MORB-like assemblages in the Paleoproterozoic Flin Flon Belt, Manitoba, and the role of intra-arc extension in localizing volcanic-hosted massive sulphide deposits. Can. J. Earth Sci. 36 (11), 1767–1788.
Talbot, C.J., Alavi, M., 1996. The past of a future syntaxis across the Zagros. Geol. Soci. London Spec. Publ. 100 (1), 89–109.
Tornos, F., Peter, J.M., Allen, R., Conde, C., 2015. Controls on the siting and style of volcanogenic massive sulphide deposits. Ore Geol. Rev. 68, 142–163.
Wilkin, R.T., Barnes, H.L., 1997. Formation processes of framboidal pyrite. Geochim. Cosmochim. Acta 61 (2), 323–339.
Winchester, J.A., Floyd, P.A., 1977. Geochemical discrimination of different magma series and their differentiation products using immobile elements. Chem. Geol. 20, 325–343.
Yarmohammadi, A., Rastad, E., Mohajjel, M., Shamsa, M.J., 2008. Barika gold mineralization, a gold-rich volcanogenic massive sulfide de-posit in Iran. J. Sci. Univ. Tehran 34 (1), 47–61.
Zohrehbakhsh, A., Vahdati Daneshmand, F., Djokovic, I., Dimitrijevic, M.D., 1990. Geology Map of Rafsanjan, Scale 1:250,000. Geological Survey of Iran.